ESTIMATION OF KINETIC PARAMETERS FOR ACETIC ACID CONVERSION TO ETHANOL

A Project Report

submitted by

MAHULA SANTRA (R670215006)

in partial fulfilment of the requirements
for the award of the degree of

MASTER OF TECHNOLOGY
(CHEMICAL ENGINEERING)
Specialization in
PROCESS DESIGN ENGINEERING

Under the guidance of

Mr. Pranab Kumar Rakshit
Manager
R & D Centre
Bharat Petroleum Corporation Limited
Greater Noida

Ms. Leena Kapoor & Dr. P. Vijay
Assistant Professor (SS) & Associate Professor
Department of Chemical Engineering
University of Petroleum and Energy Studies
Bidholi, Dehradun

DEPARTMENT OF CHEMICAL ENGINEERING

COLLEGE OF ENGINEERING STUDIES

UNIVERSITY OF PETROLEUM & ENERGY STUDIES
Bidholi Campus, Energy Acres,
Dehradun-248007.

April - 2017

DECLARATION BY THE SCHOLAR

I here by declare that this submission is my own and that, to the best of my knowledge and belief, it contains no material previously published or written by another person nor material which has been accepted for the award of any other Degree or Diploma of the University or other Institute of Higher learning, except where due acknowledgement has been made in the text.

MAHULA SANTRA (R670215006)

CERTIFICATE

This is to certify that the thesis titled **ESTIMATION OF KINETIC PARAMETERS FOR ACETIC ACID CONVERSION TO ETHANOL** submitted by MAHULA SANTRA (R670215006), to the University of Petroleum & Energy Studies, for the award of the degree of **MASTER OF TECHNOLOGY** in Chemical Engineering is a bonafide record of project work carried out by him/her/them under my/our supervision and guidance. The content of the thesis, in full or parts have not been submitted to any other Institute or University for the award of any other degree or diploma.

Mr. Pranab Kumar Rakshit
Manager

Ms. Leena Kapoor & Dr. P. Vijay
Assistant Professor (SS) & Associate Professor

Date: _____

ACKNOWLEDGEMENTS

I am thankful to **The Chemical Engineering Department, UPES, Dehradun** and **Mr. Sanjay Bhargava, General Manager, Bharat Petroleum Corporation R & D Centre, Greater Noida** for giving me this opportunity to work on a live industrial problem at BPCL R & D, Greater Noida. I would like to express my special appreciation and thanks to my project guide, **Mr. Pranab Kumar Rakshit, Manager, BPCL R & D, Greater Noida** for giving me this interesting topic to work on. His exemplary guidance, monitoring, utmost patience and enthusiasm have helped me at every step throughout.

I express my sincere gratitude to **Dr. P. Vijay, HoD, Chemical Engineering Department, UPES** and **Mr. Vinod Kumar, BPCL R & D, Greater Noida** for their kind guidance and help for the successful completion of this project.

I acknowledge **Dr. M. Gopinath, Assistant Professor (SG), Department of Chemical Engineering, UPES**, who spent his valuable time and gave me an immense support and guidance during the project period.

I am thankful to **Ms. Leena Kapoor, Assistant Professor (SS), Chemical Engineering Department, UPES**, who extended her support possible to carry out this project as an internal guide.

Many thanks to **Dr. C. Samanta, Dr. S. Pai, Dr. K. Munnusamy, Ms. R. Arundhati, Ms. Shayanti Ghosh and Ms. Sonal Asthana, BPCL R & D, Greater Noida** for familiarising and helping me with the operation of different lab instruments/equipments used for characterization, analysis and evaluation and guiding me in analyzing all the samples and interpret the results.

I am thankful to Avishek, Vishal and Rajkumar without whose help I wouldn't have carried out the laboratory experiments so easily.

I would like to extend my thanks to Mr. Varaha Prasad who provided inspiration and support during this project period.

A special thanks to my family and friends for all the sacrifices you've made on my behalf and providing me with all good things outside the work.

20 April, 2017 **MAHULA SANTRA**

NOMENCLATURE

CO_X	Carbon oxides
NO_X	Nitrogen oxides
SO_X	Sulphur oxides
PM	particulate matters
GHG	Greenhouse gases
GOI	Government of India
EURO(-III and IV)	European Emission Standards
BS	Bharat Stage Emission Standards
EBP	Ethanol Blending Program
kg	kilogram
Mt	Metric tonnes
SiO_2	Silicon dioxide
BET	Brunauer-Emmett-Teller
XRD	X-Ray diffraction
SEM	Scanning Electron microscopy
TGA	Thermo gravimetric analysis
TPR	Temperature programmed reduction
Pt	Platinum
TiO_2	Titanium dioxide
WHSV	weight hourly space velocity
In_2O_3	Indium oxide
MPa	Megapascal
hr	hour
K	Kelvin
$Co(NO_3)_2.6H_2O$	Cobalt Nitrate hexahydrate
$Pt(NH_3)_4(NO_3)_2$	Tetraamine platinum nitrate
ml	mililitre
Mol. wt.	Molecular weight
mm	millimeter
TCD	thermal conductivity detector
FID	a flame ionization detector

NLPH	net liquid per hour
kV	kilovolt

ABSTRACT

In view of being a significant contributor to Greenhouse gases, India has decided to use ethanol as a substitute to conventional petroleum fuel, however the current feedstock molasses standalone would not be able to meet the mandated requirement. Catalytic hydrogenation of acetic acid to ethanol is a promising route, superior to homogeneous and heterogeneous catalytic processes. The process of ethanol production via catalytic hydrogenation is well suited for countries like India, with limitation in farm land and a demanding target to fulfill the need of fuel.

Typically noble metal based catalysts are used for the process, of which bimetallic catalysts incorporated with Pt are the most effective. In the present work, SiO_2 supported Co and Co-Pt catalysts have been prepared by impregnation method and their characterizations have been carried out by scanning electron microscopy, BET surface area, X-ray diffraction, thermogravimetric analysis and temperature programmed reduction. The activity studies of these catalysts have been carried out in the temperature range of 240-320°C, at pressure 20 bar, at fixed flow rates of acetic acid and hydrogen, in a fixed bed catalytic reactor.

Activity of SiO_2 supported 2.1%Pt-1.8%Sn catalyst have also been studied in the temperature range of 270-310°C, varying pressure in the range of 1-20 bar, WHSV in the range of 2-4 and molar ratio of H_2 to acetic acid in the range of 3-7. Reaction models that correlate these data involving Langmuir-Hinshelwood type catalytic sequence have been derived. Several rate expressions have been derived by assuming different elementary reactions as the rate determining steps. Once the expressions developed, experimental data obtained has been used to fit these expressions. The one having the closest fit has been considered as the rate expression for the reaction. Detailed MATLAB based code has been developed to estimate the rate parameters. Finally, an attempt has been made to develop the fixed bed reactor model using the developed kinetics.

Keywords: Co-Pt catalyst preparation, characterization, Acetic acid hydrogenation, ethanol, kinetics, fixed bed reactor model

TABLE OF CONTENTS

CERTIFICATE iii

ACKNOWLEDGEMENTS iv

ABSTRACT vii

1 INTRODUCTION 1

1.1 India's Bio-fuel Policy 1

1.2 Processes of Ethanol production 2

1.3 Current Scenario of Ethanol Production, Supply and Consumption in India 2

1.4 Aim of the Project 3

2 LITERATURE REVIEW 4

2.1 Introduction to Catalysis 4

2.1.1 Catalytic Reaction 4

2.1.2 Heterogeneous catalytic theory 5

2.1.3 Components of a solid catalyst 6

2.2 Catalyst preparation 7

2.3 Ethanol production from syn-gas 7

2.4 Effect of Catalysts on Acetic acid Hydrogenation 9

2.5 Kinetics Study 10

3 MATERIALS AND METHODOLOGY 14

3.1 Chemicals 14

3.2 Equipments and Instruments 14
3.3 Preparation of Catalysts 15
3.4 Characterization of Catalysts 18
3.4.1 Surface area measurement (BET method) 18
3.4.2 X-Ray diffraction (XRD) analysis 18
3.4.3 Temperature programmed reduction (TPR) 19
3.4.4 Thermo gravimetric analysis (TGA) 19
3.4.5 Scanning Electron microscopy(SEM) 19
3.5 Performance testing of Catalysts 19
3.5.1 Experimental Set up 19
3.5.1.1 Feeding Section 19
3.5.1.2 Reactor Section 21
3.5.1.3 Product Separation Section 22
3.5.1.4 Product analysis Section 23
3.5.2 Experimental procedure 23
3.5.2.1 Catalyst loading in the reactor 23
3.5.2.2 Leakage test in the Reactor 23
3.5.2.3 Catalyst Activation 24
3.5.3 Design of Experiments 24

4 RESULTS AND DISCUSSION 26

4.1 Preparation of catalysts 26
4.2 Characterization studies 26
4.2.1 Surface properties of CP catalysts 27
4.2.2 Crystalline properties of CP catalysts 28
4.2.3 Reducibility of CP catalysts 28
4.2.4 Weight loss of CP catalysts 29

4.2.5 Morphology of CP catalysts 29
4.3 Activity of CP catalysts 30
4.3.1 Study on CP1 catalyst 30
4.3.2 Study on CP4 catalyst 31
4.3.3 Study on CP6 catalyst 31
4.3.4 Effect of CP catalysts in acetic acid hydrogenation to ethanol . 32

5 KINETICS ON ACETIC ACID CONVERSION TO ETHANOL 36
5.1 Catalyst preparation 36
5.2 Study on catalyst activity 36
5.3 Performance of the catalyst 37
5.3.1 Effect of temperature 37
5.3.2 Effect of WHSV 37
5.3.3 Effect of pressure 38
5.3.4 Effect of molar ratio of feed 38
5.4 Kinetic study 39
5.4.1 Determination of reaction rate expresssions 39
5.4.2 Estimation of Kinetic parameters 44
5.4.3 Modeling of reactor 44
5.5 Results and Discussion 45
5.5.1 Estimated values of the various kinetic parameters 45
5.5.2 Comparison between experimental conversion and simulated conversion 46
5.5.3 Variation in the flow rates of feed and products along the reactor 47

6 CONCLUSIONS 50

REFERENCES 54

APPENDIX 1 **55**

APPENDIX 2 **58**

LIST OF TABLES

3.1 Compositions of the synthesized CP catalysts 17

4.1 Properties of CP catalysts 27

4.2 TPR data of the CP catalysts 29

4.3 Lab conversion data for CP1 catalyst 33

4.4 Lab conversion data for CP4 catalyst 33

4.5 Lab conversion data for CP6 catalyst 34

5.1 Lab conversion data of SiO_2 supported Pt-Sn catalyst 37

5.2 Estimated kinetic parameters 46

5.3 Comparison study between experimental and simulated conversion . . . 46

LIST OF FIGURES

1.1 Production, Supply and Consumption rate of Ethanol in India 3

2.1 Comparison of activation energies of catalytic and non-catalytic reactions 5

2.2 Steps in a solid catalytic reaction 6

2.3 Outline of catalyst preparation step-by-step 8

2.4 Scheme of different approaches for Ethanol synthesis from syngas . . . 9

3.1 Weight balance 14

3.2 Metal solution in a measuring cylinder 15

3.3 Stirrer 15

3.4 Impregnated CP Catalyst supported on SiO_2 (standing at room temperature for 140 mins) 16

3.5 Removal of solvent from the catalyst using Rotavapor 16

3.6 petri dish containing dried catalysts 17

3.7 Furnace, which is used for catalysts drying 17

3.8 Catalysts inside tubular reactor in calcinier 18

3.9 Overview of the experimental set up 20

3.10 Catalyst loading in the reactor 24

4.1 CP Catalysts supported on SiO_2 (after removal of solvents) 26

4.2 Calcined CP catalysts 27

4.3 XRD images of calcined CP catalysts 28

4.4 H_2-TPR profile of calcined CP catalysts 30

4.5 TGA profile of CP catalysts 31

4.6 SEM images of calcined CP catalysts at 10kV 32

4.7 Effect of temperature on the performance of CP1 catalyst 33

4.8 Effect of temperature on the performance of CP4 catalyst 34

4.9 Effect of temperature on the performance of CP6 catalyst 35

4.10 Comparison of activities among CP1, CP4 and CP6 catalysts at 240°C . 35

5.1 Effect of temperature on acetic acid conversion and products selectivity at P=1 bar, WHSV=3/hr, feed molar ratio=7 38

5.2 Effect of WHSV on acetic acid conversion and products selectivity at T=270°C, P=1 bar, feed molar ratio=7 39

5.3 Effect of pressure on acetic acid conversion and products selectivity at T=270°C, WHSV=3/hr, feed molar ratio=7 40

5.4 Effect of feed molar ratio (H_2:Acetic acid) on acetic acid conversion and products selectivity at T=270°C, P=10 bar, WHSV=3/hr 41

5.5 Experimental values of acetic acid conversion *versus* predicted values of acetic acid conversion 47

5.6 Variation of acetic acid, acetaldehyde,ethanol and ethyl acetate flow rates along the reactor at 270°C 48

5.7 Variation of acetic acid, acetaldehyde,ethanol and ethyl acetate flow rates along the reactor at 290°C 48

5.8 Variation of acetic acid, acetaldehyde, ethanol and ethyl acetate flow rates along the reactor at 310°C 49

CHAPTER 1

INTRODUCTION

In today's world of rising carbon emission, ethanol, being a particulate-free burning fuel, is gaining immense importance as an alternative automotive fuel. It has attracted the attention in countries like India which, spending a huge amount of the annual budget, is heavily dependent on the import of crude oil and its refining processes. Gasoline or petrol, the most commonly used transport fuel, is a highly volatile hydrocarbon derived from crude oil. When this gasoline is blended with ethanol, it emits reduced quantities of carbon oxides (CO_X), nitrogen oxides (NO_X), sulphur oxides (SO_X) and particulate matters (PM) after combustion, compared to that of gasoline alone because ethanol acts as an oxidizing agent.

1.1 India's Bio-fuel Policy

The continuous rise in transportation and subsequent optimization in petroleum dissipation is hiking the environmental concerns. As, presently, India is the fourth largest global contributor to emission of Greenhouse gases (GHG), the Government of India (GOI) is contemplating European Emission Standards (EURO)-III and IV as reference emission norms for vehicles, which in turn feel necessity for embracement of clean and green fuels.

As of now, Bharat Stage Emission Standards (BS)-III norms are enforced across the country while BS- IV (equivalent to EURO-IV) norms have been imposed across only 14 major cities (Delhi, Mumbai, Kolkata, Chennai, Bengaluru, Hyderabad, Ahmedabad, Pune, Surat, Kanpur, Lucknow, Sholapur, Jamshedpur and Agra). To conform that goal, the Union Cabinet implemented the National Policy on Biofuels on December 24, 2009, which enlivens use of renewable energy resources as alternative fuels to complement transport fuels. Further, a significant target to substitute 20% of petroleum fuel utilization with bio-fuels (bio-ethanol and bio-diesel) by the end of Calendar Year 2017 has been proposed.

In a bid to extend the target and actively resolve the "Ethanol Blending Program" (EBP), the GOI recommended 10% compulsory blending of ethanol with gasoline across all states (Mustard and Aradhey, 2012).

1.2 Processes of Ethanol production

Traditionally, ethanol is mainly produced by two routes:

(i) fermentation of biomass, especially sugars that containing six carbons, and

(ii) hydration of ethylene, which is based on petroleum industry (Solomon *et al.*, 2007; Subramani and Gangwal, 2008)

The ethylene hydration process, which is carried out by reacting ethylene with steam at 300°C, 6-7 MPa over a solid catalyst, can get industrial-grade pure ethanol. The challenge for this route of ethanol production confronted is the rising of crude oil price and the dependence on imported oil (Fougret and Hölderich, 2001). The fermentation process is unsuitable for woody biomass and sugars derived lignocelluloses and the crude product contains only about 14% pure ethanol (Rostrup-Nielsen, 2005).

Alternatively, recent studies say that ethanol can be synthesized from syngas via catalytic processes (Subramani and Gangwal, 2008).

1.3 Current Scenario of Ethanol Production, Supply and Consumption in India

India, the world's second largest sugarcane producer, produces mainly molasses-derived ethanol by the fermentation process. Since production of sugarcane is cyclical in India, ethanol production also differs consequently and hence, sometimes, does not assure optimal contribution levels needed to meet the requirements. At times, availability of sugar molasses at a lower rate leads to increased price of the feedstock and ultimately alters the cost of ethanol production, thereby agitating the supply of ethanol for the blending program at pre-negotiated fixed ethanol prices.

It is estimated that 85-100 kg of sugar (8.5-10%) and 35-45 kg (3.5-4.5%) of molasses can be obtained from 1 tonne of sugarcane whereas the recovery of ethanol from molasses is 22-25%, as per Indian standards. Theoretically, if the entire sugarcane crop (342.4 Mt in 2010-11) is used for sugar production, estimated molasses production is 15.4 Mt, and the associated estimated ethanol yield is 3.6 billion litres. In reality, only 70-80% of sugarcane produced in India is used for sugar production, and the remaining is used for other applications like alternative sweeteners (jiggery and khandsari) and seeds. Moreover, 32.5% of the available molasses is used in alcoholic beverages, 25% by industry, and

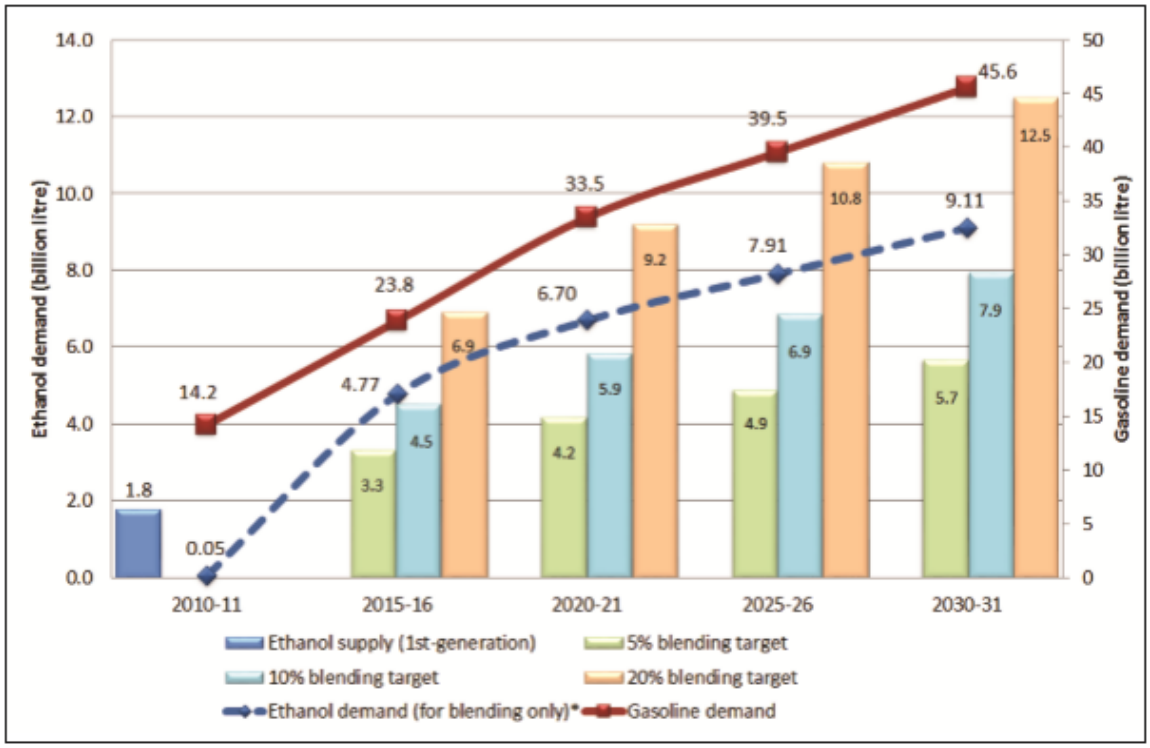

**with 20% blending target*

Figure 1.1: Production, Supply and Consumption rate of Ethanol in India

3.5% for other applications. The remaining available alcohol is diverted for blending with transportation fuel (Mustard and Aradhey, 2012).

Fig. 1.1 shows the production, supply and consumption rate of ethanol in India.

1.4 Aim of the Project

The present project aims at the preparation of SiO_2 supported Cobalt and Cobalt-Platinum catalysts alongwith a study on their characterizations (by BET surface area, XRD, SEM, TGA and TPR) and activity testing for acetic acid conversion to ethanol by hydrogenation.

A detailed study on mechanism of chemical kinetics during this hydrogenation process and estimation of the kinetic parameters are further aimed.

CHAPTER 2

LITERATURE REVIEW

2.1 Introduction to Catalysis

The interdisciplinary area involving the ambit of thermodynamics, electronic interaction, crystal structure, reactor design and process development for a catalytic process is a simple denition for catalysis, which involves contributions from chemical engineers for process development, chemists for the ecacy of the catalyst structure and material scientists for fundamental structural studies, and thus it is a vast area spanning preparation of catalysts to nal utilization in a chemical reactor.

2.1.1 Catalytic Reaction

A catalyst is a substance which increases the rate of attaining chemical equilibrium in a reaction without the substance itself not undergoing any net consumption. A catalyst accelerates both the rates of the forward and reverse reaction. Equilibrium of a reversible reaction is not altered by the presence of the catalyst. In a thermodynamically feasible chemical reaction, when addition of a catalyst increases the rate of attainment of chemical equilibrium but the substance itself does not undergo any chemical change, then the reaction is called a catalytic reaction (Fogler, 2006).

Catalysts work by providing alternative mechanism involving a different transition state of lower energy. Thereby, the activation energy of the catalytic reaction is lowered compared to the uncatalyzed reaction (Ref. Fig. 2.1).

Catalytic reactions can be of two types:

1. Homogeneous catalytic reaction, involving with process in which a catalyst is in solution with at least one of the reactants.
2. Heterogeneous catalytic reaction,that involves more than one phase- usually the catalyst is a solid and the reactants and products are in liquid or gaseous forms.

Catalysis play a critical role in the Chemical industry, and given pressing eco-efficient and financial demand, it is estimated that over 90% of Chemical commercial processes

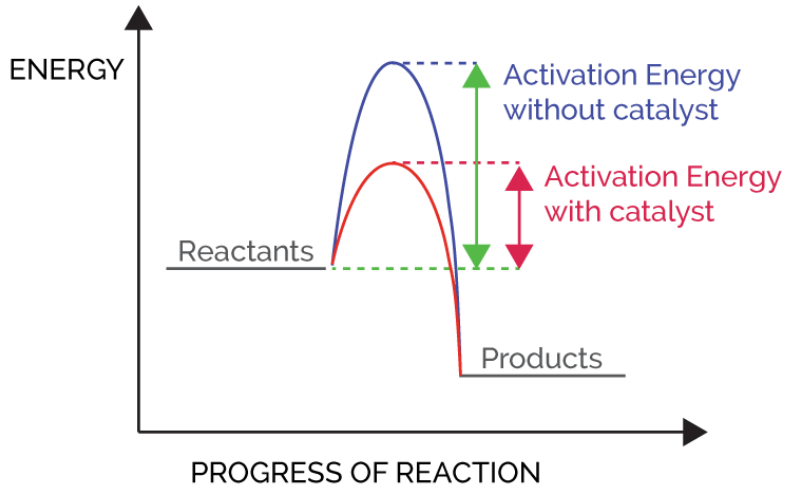

Figure 2.1: Comparison of activation energies of catalytic and non-catalytic reactions

involve a catalytic component. Of all the industrial catalytic processes, approximately 80% involve the use of solid catalysts, 17% homogeneous catalysts and rest 3% biocatalysts. Thus, heterogeneous catalysts, particularly solid catalysts, dominate the industrial catalytic processes (Fogler, 2006).

2.1.2 Heterogeneous catalytic theory

Of the entire surface, only the active sites are known to be responsible for catalyzing reactions. These can be understood as unsaturated atoms resulting from surface irregularities or atoms with chemical properties that enable the interaction with the adsorbed reactant atoms or molecules. Activity of the catalyst is directly proportional to the number of these active sites available on the surface and is often expressed in terms of turnover frequency. Turnover frequency is defined as the number of molecules reacting per active site per second at the condition of experiments (Fogler, 2006).

A heterogeneous catalytic reaction

$$A \rightarrow B \tag{2.1}$$

proceeds through the following steps, the steps are illustrated in Fig. 2.2.

1. Transportation of reactant (A) from the bulk fluid to the external surface of the pellet.
2. Diffusion of reactant (A) into the interior of the pellet.
3. Adsorption of reactant (A) into the interior of the pellet.

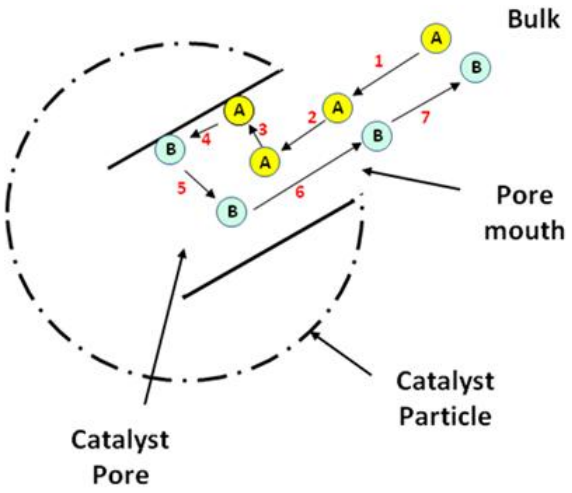

Figure 2.2: Steps in a solid catalytic reaction

4. Reaction of reactant (A) to form B.
5. Desorption of product (B) from the surface.
6. Diffusion of product (B) from the pellet interior to the external surface.
7. Transport of product (B) away from the solid surface to the bulk fluid.

The overall rate of reaction is equal to the rate of slowest step in the mechanism. When the mass transfer and diffusion steps (1, 2, 6, 7) are very fast compared to adsorption and reaction steps (3, 4, 5), concentration in the immediate vicinity of the active sites is the same or indistinguishable from that in the bulk fluid.

Consequently, the transport or diffusion steps do not affect the overall rate of the reaction. Alternatively, if reaction and diffusion steps are fast compared to the mass transfer steps, then mass transfer does affect the rate of reaction. When mass transfer from the bulk phase to the pore mouth is slow and affects the reaction rate, then changing the flow conditions past the catalyst should change the overall reaction rate. In case of porous catalysts, diffusion within the catalyst pores may limit the reaction rate. Under this condition external flow does not affect the reaction rate but internal diffusion does affect (Fogler, 2006).

2.1.3 Components of a solid catalyst

A solid catalyst consists of mainly three components (Fogler, 2006), as follows

1. Catalytic agent : These are the catalytically active components that generate the active sites which participate in the chemical reaction. Activity of any catalyst is

proportional to the concentration of these active sites. Though concentration of the active sites depends on the amount of catalytically active component, however, it is not always directly proportional. Availability of active sites depends mainly on the dispersion of catalytic agent. The dispersion is defined as ratio of total number of exposed atoms/molecules of catalytic agent available for reaction to total number of atoms/molecules of catalytic agent present in the catalyst sample. Catalytic agents may be metallic conductors or semiconductors or insulators.

2. Support /carrier : Support or carrier provides large surface area for dispersion of small amount of catalytically active agent. This is particularly important when expensive metals, such as platinum, ruthenium, palladium or silver are used as the active agent. Supports give the catalysts its physical form, texture, mechanical resistance and certain activities.

   Support may be inert or interact with the active component. This interaction may result in change in surface structure of the active agent and thereby affect the catalyst activity and selectivity. The support may also exhibit ability to adsorb reactant and contribute to the reaction process.

   Hence, supported catalysts are those catalysts in which the catalytically active materials are dispersed over the high surface area support material.

3. Promoters and Inhibitors : Promoters are generally defined as substances added during preparation of catalysts that improve the activity or selectivity or stabilize the catalytic agents. The promoter is present in a small amount and by itself has little or no activity.

2.2 Catalyst preparation

Catalysts can be prepared by various techniques (Perego and Villa, 1997), among which impregnation method is discussed in this section.

Impregnation process is an important method of catalyst preparation, in which supports are first prepared by bulk preparation methods and then impregnated with the catalytically active material. The active materials, again, can be deposited on the supports by many different methods. Most of the methods involve aqueous solutions and liquid solid interface. In some cases, deposition is done from the gas phase and involves gas- solid interface.

2.3 Ethanol production from syn-gas

Ethanol production through direct approach of syngas-to-ethanol, because of the availability of syngas from coal, biomass and natural gas (including conventional natural gas

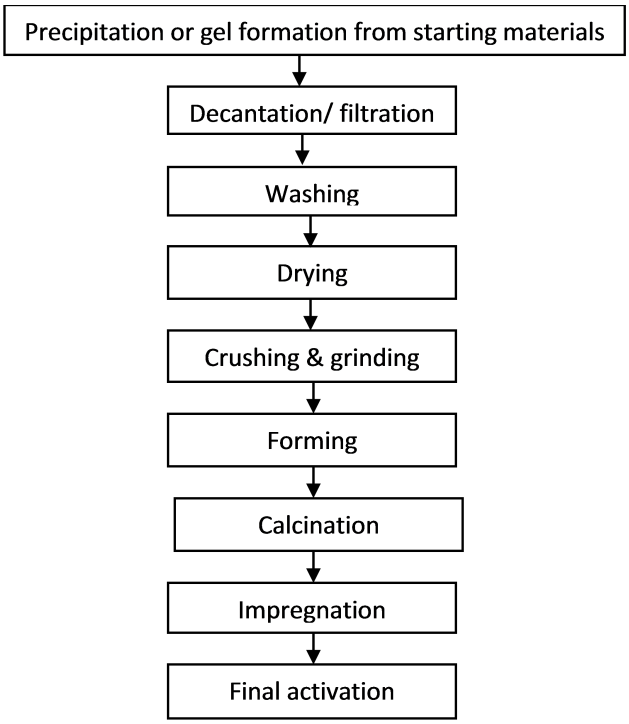

Figure 2.3: Outline of catalyst preparation step-by-step

and unconventional gases such as shale gas, coal bed gas and tight gas), has drawn a great deal of attention since few years (Choi and Liu, 2009; Haider *et al.*, 2009; Pan *et al.*, 2007; Subramani and Gangwal, 2008). But, this process has unsolved drawbacks, including low conversion and poor selectivity of ethanol.

Dimethyl oxalate hydrogenation or combined carbonylation of dimethyl ether and hydrogenation of methyl acetate - both produces ethanol (Gong *et al.*, 2012; Yang *et al.*, 2011); but, again, lower selectivity or overall atomic efficiency exists in either of these two processes which are the main disadvantages.

Technology of acetic acid synthesis has been well developed through methyl carbonylation (Howard *et al.*, 1993; Sunley and Watson, 2000) and the global acetic acid had an overcapacity of more than 40% in 2010.

Also, acetic acid can be made from syngas in the presence of supported metallic catalysts (Chen *et al.*, 2006; Xu, 1998). Hence, an alternative process for ethanol synthesis via syngas is through selective hydrogenation of acetic acid (Kiff and Schreck, 1983; Verser and Eggeman, 2003). Fig. 2.4 represents Scheme of different approaches for Ethanol synthesis from syngas

This process is a consolidated technology which consists of the conversion of syngas to methanol, coupling with CO to form acetic acid, and subsequent hydrogenation to form

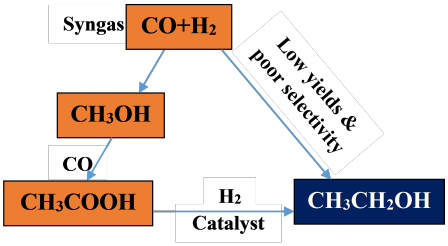

Figure 2.4: Scheme of different approaches for Ethanol synthesis from syngas

ethanol. Many noble metal-based catalysts have the capacity of catalyzing the process of different acids getting converted to alcohols (Aly and Baumgarten, 2001; Miyake *et al.*, 2009). However, lower ethanol selectivity or harsh reaction conditions is suffered by most of these catalysts. Therefore, more detailed studies on the correlation between catalyst structure and performance are very necessary.

2.4 Effect of Catalysts on Acetic acid Hydrogenation

It has been reported that conversion of acetic acid to ethanol via hydrogenation can be easily consummated over Pt-, Ru-, Pd-based catalysts based on the calculations and experiments of density functional theory (Alcala *et al.*, 2005; Olcay *et al.*, 2010; Pallassana, 2002; Rachmady and Vannice, 2002, 2000).

In an work, bimetallic catalysts have been demonstrated to be very eective for the hydrogenation of acetic acid followed by its conversion to ethanol. An investigation on catalytic behaviour of acetic acid hydrogenation over Platinum supported on TiO_2, SiO_2, Al_20_3 and Fe_20_3 has indicated that the reaction involves both metal and oxide support and it takes place at sites on the oxide surface. The catalysts involved in this reaction were prepared by using incipient wetness mechanism after being calcined at 773 K at first for 2 hrs of compressed air to remove any impurity. The platinum salt solution was added dropwise to the calcined oxide support and after complete addition, they were dried under 393 K for an overnight. Pt/TiO_2 catalyst (at 420K) have been seen to be the most active for acetic acid hydrogenation of 5% and giving the highest selectivity to ethanol, up to 70%

There are a number of patents which indicate that bimetallic catalysts incorporated with Pt are very effective for the hydrogenation of acetic acid followed by its conversion to ethanol. An investigation on the catalytic behaviour of acetic acid hydrogenation over Platinum (Pt) supported on titanium dioxide (TiO_2), silicon dioxide (SiO_2), aluminum oxide (Al_20_3), and ferric oxide (Fe_20_3) have been reported where a strong evidence is obtained that the reaction involves both metal (Pt) and oxide support, and it takes place at

sites on the oxide surface. Pt/TiO_2 catalyst has been seen to be the most active for acetic acid hydrogenation than the other Pt catalysts, and Pt/TiO_2 catalyst has given the highest selectivity to ethanol, up to 70 % (Rachmady and Vannice, 2000).

The carbon nanotube-supported bimetallic Pt-Sn catalyst showed the best performance, exhibiting over 97% conversion and 92% selectivity to ethanol under conditions of 350, 2.0 MPa pressure, weight hourly space velocity (WHSV)=1.5/hr and feed ratio=80 (Zhang *et al.*, 2013).

It has been disclosed that ethanol can be formed from acetic acid over a ruthenium catalyst at extremely high pressures of 700-950 bars in order to achieve yields of around 88%, whereas low yields of only about 40% are obtained at pressures of about 200 bar. Nevertheless, both of these conditions are unacceptable and uneconomical for a commercial operation (Ford, 1952).

It has been reported that at 21 bar pressure in the temperature range 220-380°C, in the presence of alumina supported nickel catalyst hydro-conversion of acetic acid to ethanol occurs and the yield of ethanol gets increased drastically by addition of In_2O_3 (Onyestyák *et al.*, 2013).

It has also been disclosed and claimed that by vapor phase reaction of acetic acid over either cobalt and palladium supported on graphite catalyst or cobalt and platinum supported on silica catalyst selectively produces ethanol at a temperature of about 250°C (Johnston *et al.*, 2013).

2.5 Kinetics Study

Heterogeneous catalytic processes of acetic acid hydrogenation to ethanol results into unsolved drawbacks like low conversion and poor selectivity of ethanol due to the slow formation kinetics of the C-C bond and the fast chain growth of the C_2 intermediates, the process (Pan *et al.*, 2007; Rachmady and Vannice, 2002).

Kinetics study on ethanol production from acetic acid hydrogenation has been conducted by several authors (Onyestyák *et al.*, 2013; Pestmam *et al.*, 1997; Rachmady and Vannice, 2002, 2000).

It has been reported that the following observations can be made about the kinetic behavior of acetic acid hydrogenation to form organic compounds over TiO_2 supported Pt catalysts (Rachmady and Vannice, 2000):

1. The reaction requires both metal and an oxide phase in the catalyst.

2. Oxides that are active for ketonisation are the best supports, implying the reaction can occur on the oxide surface.

3. The metal, Pt, acts as a source of activated hydrogen, presumably hydrogen atoms.

4. For Pt/TiO_2 the reaction orders varied between 0.2 and 0.4 with respect to acetic acid and between 0.4 and 0.6 with respect to hydrogen.

5. The apparent activation energy is affected by both H_2 and acetic acid partial pressures.

Based on these statements, various reaction models have been considered for the hydrogenation of acetic acid to form acetaldehyde, ethanol, and ethane over Pt/TiO_2 catalysts, and a Langmuir-Hinshelwood-type catalytic sequence provided a derived rate expression that gave the most consistent fit. The surface reactions and reversible desorption steps are depicted by Eqns. 2.6 - 2.14 in the following sequential elementary steps:

$$H_{2(g)} + 2^* \leftrightharpoons 2H^* \tag{2.2}$$

$$H^* \leftrightharpoons H_{sp} \tag{2.3}$$

$$CH_3COOH_{(g)} + 2^* \leftrightharpoons CH_3COO^* + H^* \tag{2.4}$$

$$CH_3COOH_{(g)} + S \leftrightharpoons CH_3COOH - S \tag{2.5}$$

$$CH_3COOH - S + H_{sp} \leftrightharpoons CH_3COOH_2 - S \tag{2.6}$$

$$CH_3COOH_2 - S + H_{sp} \leftrightharpoons CH_3CHO - S + H_2O \tag{2.7}$$

$$CH_3CHO - S \leftrightharpoons CH_3CHO_{(g)} + S \tag{2.8}$$

$$CH_3CHO - S + H_{sp} \leftrightharpoons CH_3CHOH - S \tag{2.9}$$

$$CH_3CHOH - S + H_{sp} \leftrightharpoons CH_3CH_2OH - S \tag{2.10}$$

$$CH_3CH_2OH - S \leftrightharpoons CH_3CH_2OH_{(g)} + S \tag{2.11}$$

$$CH_3CH_2OH - S + H_{sp} \leftrightharpoons CH_3CH_2OH_2 - S \tag{2.12}$$

$$CH_3CH_2OH - S + H_{sp} \leftrightharpoons CH_3CH_3 - S + H_2O_{(g)} \tag{2.13}$$

$$CH_3CH_3 - S \leftrightharpoons CH_3CH_{3(g)} + S \tag{2.14}$$

The hydrogenation activity is determined by the rate of acetic acid disappearance to form hydrogenated products, i.e., the overall rate of formation of acetaldehyde, ethanol, and

ethane, as shown in Eqn. 2.15:

$$r_{HOAc} = r_{acetaldehyde} + r_{ethanol} + r_{ethane} \tag{2.15}$$

It follows from Eqs. 2.8, 2.11 and 2.14 that the rates of formation of these products can be expressed as:

$$r_{acetaldehyde} = k_3\theta_{acetaldehyde} - k_{-3}P_{acetaldehyde}\theta_S \tag{2.16}$$

$$r_{ethanol} = k_6\theta_{ethanol} - k_{-6}P_{ethanol}\theta_S \tag{2.17}$$

$$r_{ethane} = k_9\theta_{ethane} - k_{-9}P_{ethane}\theta_S \tag{2.18}$$

where θ_i is the fractional surface coverage of species i, with S representing an empty site, and P_i is the partial pressure of species i. Applying the steady-state approximation to the surface intermediates, it can be easily shown that

$$r_{HOAc} = k_1\theta_A C_H \tag{2.19}$$

where HOAc represents acetic acid, the subscript A refers to the acetic acid molecules adsorbed on the oxide and C_H is the concentration of hydrogen atoms at this site on the oxide surface. The total number of active sites is incorporated in k_1. The quasi-equilibrium expressions representing adsorption on the Pt surface are:

$$K_{H_2} = {\theta_H}^2/P_{H_2}{\theta_*}^2 \tag{2.20}$$

$$K_{Ac} = \theta_{Ac}\theta_H/P_A{\theta_*}^2 \tag{2.21}$$

where subscripts * and Ac, represent vacant sites and acetate on the Pt surface, respectively. The quasi-equilibrium expressions for acetic acid adsorption and H atom concentration at the oxide surface site are written as:

$$K_A = \theta_A/P_A{\theta_*}^2 \tag{2.22}$$

$$K_{sp} = C_H/\theta_H \tag{2.23}$$

Expressions for θ_A and C_H can be obtained from Eqns. 2.20 - 2.23 and substitution into Eqn. 2.19 gives

$$r_{HOAc} = k_1 K_A K_{sp} {K_{H_2}}^{1/2} P_A {P_{H_2}}^{1/2}\theta_S\theta_* \tag{2.24}$$

where k_1 includes the active site concentration. Because adsorbed hydrogen atoms (H^*) and adsorbed acetate species ($CH3COO^*$) are the predominant surface species on Pt, a

balance on * sites gives the expression for θ^*,

$$\theta_* = \frac{1}{{K_{H_2}}^{1/2}{P_{H_2}}^{1/2} + K_{Ac}P_A/{K_{H_2}}^{1/2}{P_{H_2}}^{1/2}} \tag{2.25}$$

And, if the reaction runs at low conversion so that product concentrations are low, it can be assumed that molecular acetic acid is the only significant surface intermediate on the oxide surface sites, which gives

$$\theta_S = \frac{1}{1 + K_A P_A} \tag{2.26}$$

The final rate expression is obtained by substituting Eqns. 2.25 and 2.26 into Eqn. 2.24 to give:

$$r_{HOAc} = \frac{k_1 K_A K_{sp} {K_{H_2}}^{1/2} P_A {P_{H_2}}^{1/2}}{({K_{H_2}}^{1/2}{P_{H_2}}^{1/2} + K_{Ac}P_A/{K_{H_2}}^{1/2}{P_{H_2}}^{1/2})(1 + K_A P_A)}$$

$$r_{HOAc} = \frac{k_1^{'} P_A {P_{H_2}}^{1/2}}{(K_2 {P_{H_2}}^{1/2} + K_3 P_A/{P_{H_2}}^{1/2})(1 + K_4 P_A)} \tag{2.27}$$

where

$$k_1^{'} = k_1 K_A K_{sp} {K_{H_2}}^{1/2}; K_2 = {K_{H_2}}^{1/2}; K_3 = K_{Ac}/{K_{H_2}}^{1/2}; K_4 = K_A$$

This equation have then been fitted to the experimental data obtained from the Arrhenius and the partial pressure runs with the 0.69% Pt/TiO_2 (HTR) and 2.01% Pt/TiO_2 (LTR) catalysts using a least-squares nonlinear optimization. The iteration process initiated with a number of sets of initial values, each with initial reasonable values for all the parameters and it continued until optimum values are obtained.

The kinetics of this process is indispensable for the sizing of reactor and the research on this topic is few. It has been reported that experiments were conducted to explore the reaction mechanism of acetic acid hydrogenation, both on TiO_2 supported Pt and Pt-Fe catalysts and similar kinetics were obtained based on Langmuir-Hinshelwood-type model, which involve the dissociation of hydrogen on Pt sites along with the adsorption and activation of acetic acid on oxide phases to create surface acyl species. Catalysts used in commercial process should have appropriate pellet dimension so as to maintain a good physical strength and a suitable pressure drop. Therefore, more detailed studies on the correlation between the catalyst structure and performance are still necessary as understanding the mechanistic details of a reaction at molecular level can be an integral part of designing and developing better catalysts (Liu *et al.*, 2011).

CHAPTER 3

MATERIALS AND METHODOLOGY

3.1 Chemicals

Cobalt Nitrate hexahydrate ($Co(NO_3)_2.6H_2O$) and Tetraamine platinum nitrate ($Pt(NH_3)_4(NO_3)_2$) were purchased respectively from Acros Organics and Sigma-Aldrich Corporation. Catalyst support Silicon dioxide (SiO_2) was purchased from Saint Gobain.

3.2 Equipments and Instruments

The different equipments and instruments used during the preparation of the impregnated catalyst were:

a) Weigh balance (Fig. 3.1)- to measure the weight of the metal nitrates, catalyst support and the catalyst at every step.

Figure 3.1: Weight balance

b) Measuring cylinder (Fig. 3.2)- to measure and maintain the volume of the aqueous solutions of the metal nitrates.

c) Stirrer (Fig. 3.3)- to stir the aqueous mixture properly.

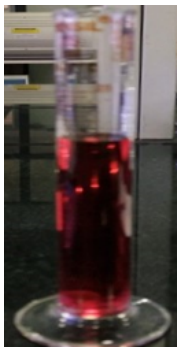

Figure 3.2: Metal solution in a measuring cylinder

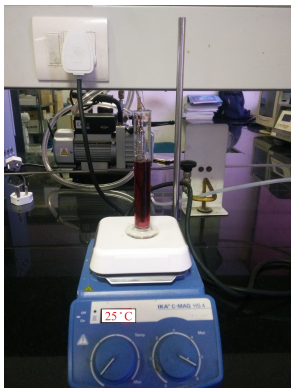

Figure 3.3: Stirrer

d) Round-bottomed flask (Fig. 3.4)- to prepare the impregnated catalyst.

e) Rotary evaporator (Fig. 3.5)- to remove the excess solvent from the impregnated catalyst.

f) Petri dish (Figure 3.6)- to keep the impregnated catalyst for drying.

g) Furnace (Fig. 3.7)- to dry the catalyst inside the furnace.

h) Tubular reactor (Fig. 3.8)- to calcine the impregnated catalyst.

i) Calcinier(Fig. 3.8) - to calcine the impregnated catalyst.

3.3 Preparation of Catalysts

SiO_2 supported Cobalt and Cobalt-Platinum catalysts were prepared by impregnation method.

A measuring cylinder (Fig. 3.2) containing 19.5 ml aqueous solution of $Co(NO_3)_2.6H_2O$ was prepared and stirred at room temperature till the properly stirred solution was achieved.

Figure 3.4: Impregnated CP Catalyst supported on SiO_2 (standing at room temperature for 140 mins)

Figure 3.5: Removal of solvent from the catalyst using Rotavapor

It was then added to a round bottomed flask containing 15 g of SiO_2 in a drop-wise manner.

After the complete addition, the impregnated catalyst inside the flask was left standing (Figure 3.4) at room temperature for around 140 minutes and subsequently was fitted to a rotary evaporator (IKA RV 10) (Fig. 3.5) for the removal of the excess solvent. The distillation time was (IKA RV 10 digital) around 35 minutes at 110 rpm, temperature set at 65°C (IKA HB 10 digital).

The distilled catalyst was left at room temperature for an overnight. Then, it was kept in furnace for drying at 150°C for 60 minutes and dried catalyst was obtained (Fig. 3.6). The catalyst was subsequently calcined under air first at 150°C for 120 minutes at rate of 5°C/min and then at 500°C at a rate of 2°C/min for 240 minutes. Finally the calcined catalyst was obtained.

Other catalysts (Table 3.1) were prepared following a similar procedure. The molecular weight percent of each metal in the catalyst, as listed in Table 3.1, represents their theoretical values. Hereafter, the catalysts are represented by the presence of metal components

Figure 3.6: petri dish containing dried catalysts

Figure 3.7: Furnace, which is used for catalysts drying

in which Co and Pt are abbreviated as C and P respectively.

Table 3.1: Compositions of the synthesized CP catalysts

Catalyst	Co(Mol. wt. %)	Pt(Mol. wt. %)
CP1	5	-
CP2	10	-
CP3	15	-
CP4	5	0.1
CP5	10	0.1
CP6	15	0.1

The percentage of Pt in the catalysts values is represented by the values in the parentheses.

The bimetallic catalysts were prepared by adding 0.0298 g $Pt(NH_3)_4(NO_3)_2$ during preparing the aqueous solution in the first step, followed by the same procedures in the next steps.

Figure 3.8: Catalysts inside tubular reactor in calcinier

3.4 Characterization of Catalysts

3.4.1 Surface area measurement (BET method)

The Brunauer-Emmett-Teller (BET) surface area of the fresh catalyst has been determined by a multipoint N_2 adsorption-desorption method at liquid-N_2 temperature using ASAP 2020 (Micromeritics, USA). Approximately 200 - 220 mg of catalyst sample was taken in a glass tube and treated (degassed) under vacuum at 300°C for 4 hours to remove the physisorbed water and adsorbed gases.

During analysis the pressure of the analysis gas (nitrogen) was maintained between 10-12 psi. The data was collected at varying partial pressures.

3.4.2 X-Ray diffraction (XRD) analysis

The power X-Ray diffraction pattern of the catalysts were obtained from PhilipsX'PertX-ray diffractometer using Copper Kα radiation source (γ=1.542) at a rate of 2.4°/min in the range 2θ=15-70°. For this study, the sample preparation involved gentle grinding of the solid into a fine powder and packing of approximately 0.5-0.8 g of powder into an aluminium sample holder with light compression to make it flat and tight.

3.4.3 Temperature programmed reduction (TPR)

The TPR measurement of the catalyst samples were performed on a Thermo Fischer Scientific TPD/R/O (1100 Series) analyzer to determine the reduction behavior of the materials. In this analysis, approximately 10-15 mg weight of sample was put in the U-tube and the sample was flushed with Ar gas at a flow rate of 30 ml/min and at 150°C for 2 hrs, following which the sample was cooled to 50°C at a rate of 10°C/min. Then the sample was heated to 900°C at a heating rate of 10°C/min in the presence of a mixture of 5.2% hydrogen in Ar.

3.4.4 Thermo gravimetric analysis (TGA)

The TGA experiments were carried out using a Perkin Elmer TGA 4000 analyzer. N_2 was used as a carrier gas at 20 ml/min and atmospheric pressure. The temperature was programmed from 40°C to 600°C at a heating rate of 10°C/min.

3.4.5 Scanning Electron microscopy(SEM)

The surface morphologies of various catalysts for ethanol synthesis were characterized by VEGA LSU (TESCAN) SEM analyzer. The images were obtained at a magnification of 200x and at 10kV using a secondary electron detector.

3.5 Performance testing of Catalysts

3.5.1 Experimental Set up

A brief description of the testing unit where the activity of catalysts for hydrogenation of acetic acid to ethanol were studied is discussed in this section. The overall plant set up (Fig. 3.9) consists of four sections: Feeding Section, Reactor Section, Product Separation Section, Product Analysis Section.

3.5.1.1 Feeding Section

This section consists of two parts: Gas feed section and Liquid feed section.

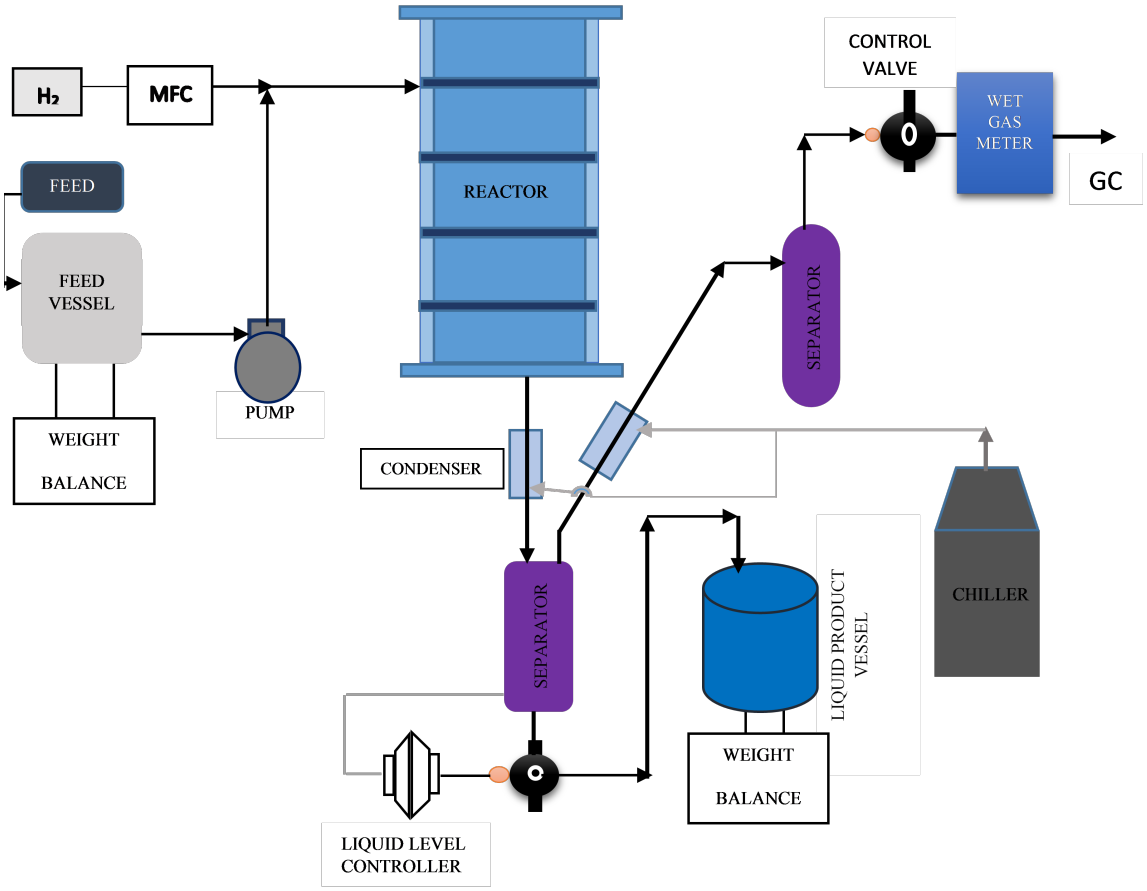

Figure 3.9: Overview of the experimental set up

Gas feed section

In the gas feed section, gas is supplied through cylinder. Mass flow controller is provided to adjust the flow of the hydrogen gas.

The H_2 gas line is equipped with following:

- One stop valve

- One filter

- One pressure regulator

- One safety relief valve

- One pressure gauge

- One mass flow meter

- One check valve

Liquid feed section

This feed section is composed of a feed tank, mounted on a weigh scale to assume a mass balance, from where liquid feed is injected at the desired rate from a feed tank mounted on a weight scale with the help of a calibrated metering pump, connected to a liquid injection line.

The injection line is equipped with the following devices:

- One stop valve

- One drain valve

- One burette to calibrate the flow rate of pump

- One high pressure positive displacement pump equipped with safety valve.

The pump is equipped with the following equipments:

- One drain valve

- One pressure gauge

- One stop valve

- One check valve

- One pressure gauge with its separator

All the component of this section is made of stainless steel.

Both the feed streams leave their designated flow controllers and are mixed together before entering the reactor.

Two pressure gauges are installed to monitor the reactor inlet and the reactor outlet pressures respectively, and the reactor outlet pressure is also monitored by a pressure transducer model made by Consolidated Controls. Temperature is maintained according to the run.

3.5.1.2 Reactor Section

Reactor type : Fixed bed tubular reactor

Reactor length : 378 mm

Reactor diameter : 25.4 mm

Maximum operating pressure : 200 bar

Maximum operating temperature: 550°C

Operating mode : Down flow mode

The inlet line to the reactor is equipped with:

- One pressure gauge

- One rupture disk

The reactor is equipped with:

- One central temperature probe with three type K thermocouples, used for internal temperature display

- One furnace with three independent control zones

The outlet line of the reactor is equipped with:

- One condenser

This condenser-equipped line is connected to the separation zone, where a high pressure separator is present.

3.5.1.3 Product Separation Section

The separator is equipped with a liquid level controller to control the liquid level in the separator. The liquid product is collected in the product vessel via one gas-liquid separator. The gaseous product from separator passes into the wet gas meter.

Separator and gas out section is equipped with the following:

- One drain valve

- One pressure gauge

- One stop valve

- One check valve

- One gas filter

- One pressure control valve

- One condenser

3.5.1.4 Product analysis Section

All the products were analyzed in a gas chromatography provided with a thermal conductivity detector (TCD), a flame ionization detector (FID) and a Molsieve and Oxyplot Column, where the lighter products are separated. Both detector and column are placed in the oven and gets operated within 0-150°C range.

The main liquid products collected were:

- Ethanol

- Ethyl acetate

- Acetaldehyde

- (unconverted) acetic acid

The gaseous products obtained were:

- Hydrogen

- Methane(negligible)

3.5.2 Experimental procedure

3.5.2.1 Catalyst loading in the reactor

12 g catalyst was loaded in the reactor as shown in figure. At the bottom, 8 mm glass wool is put, upon which 90 mm of glass beads are kept. Then the catalyst is loaded in four beds alongwith glass beds (each bed = 25 mm). Finally, at the top, glass beads of 180 mm is put.

3.5.2.2 Leakage test in the Reactor

After the catalyst is loaded in the reactor, pressure drop is studied at the pressure range the particular reaction should run (here, 1-30 bar g) in the presence of nitrogen (or hydrogen gas) gas flow at the rate of 38-40 NLPH for about 18-20 hours.

During this time, if there any pressure drop is seen, a soap solution is poured in a dropwise manner to the four joints (two with the furnace, one inlet and one outlet line) - the joint showing bubble formation implies that there is a leakage and should be checked and tightened, and the pressure drop checking procedure is repeated.

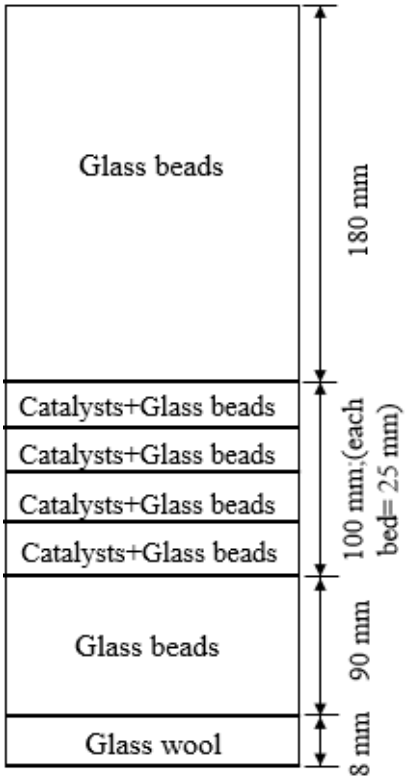

Figure 3.10: Catalyst loading in the reactor

3.5.2.3 Catalyst Activation

If there is no pressure drop, the activation of the catalysts is started for the particular range of temperature at which the reactions will be studied.

In this study, the catalyst is activated in the presence of hydrogen gas fed at the rate of 15 NLPH, at temperature increasing at the rate of 3°C/min from room temperature to 150°C, kept on hold for 180 min and then to 350°C , kept on hold for 240 min, and finally cooled to 120°C.

After catalyst activation step is over, the main experimental runs are started.

3.5.3 Design of Experiments

Hydrogen gas is supplied from hydrogen cylinder and acetic acid is pumped from the feed tank to the fixed bed catalytic reactor.

In order to estimate the ethanol production from the hydro-conversion of acetic acid and to study the effect of temperature on this process, a set of 6 experiments were designed for each CP catalysts.

The experiments were performed at a fixed pressure of 20 bar g in the temperature range of 220-320°C, at fixed flow rates of hydrogen (56 NLPH) and acetic acid (0.48 ml/min).

CHAPTER 4

RESULTS AND DISCUSSION

4.1 Preparation of catalysts

The dried solid catalysts obtained were as shown in Fig. 4.1. The catalysts after calci-

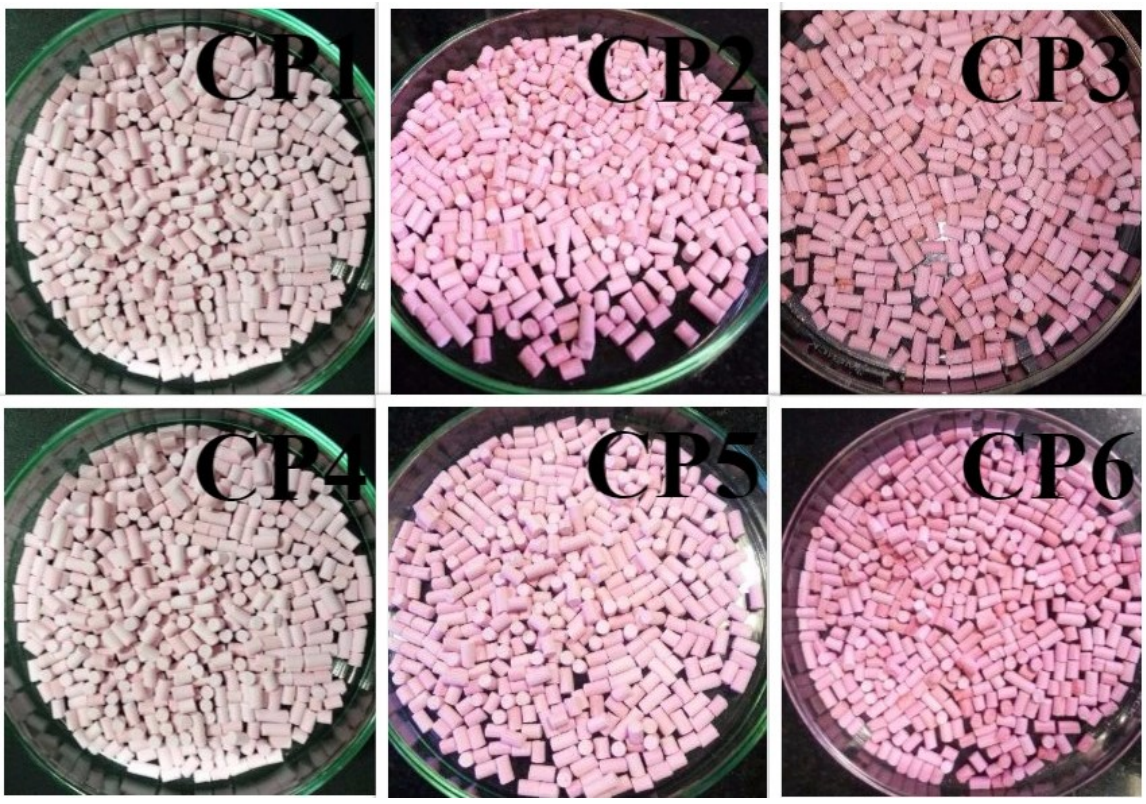

Figure 4.1: CP Catalysts supported on SiO_2 (after removal of solvents)

nation turned to black in colour as shown in Fig. 4.2, due to the reduction of metals into their oxides as a result of heating to a high temperature.

4.2 Characterization studies

The characteristics of the prepared catalysts were tested through various catalyst characterization techniques and are briefly summarized as follows:

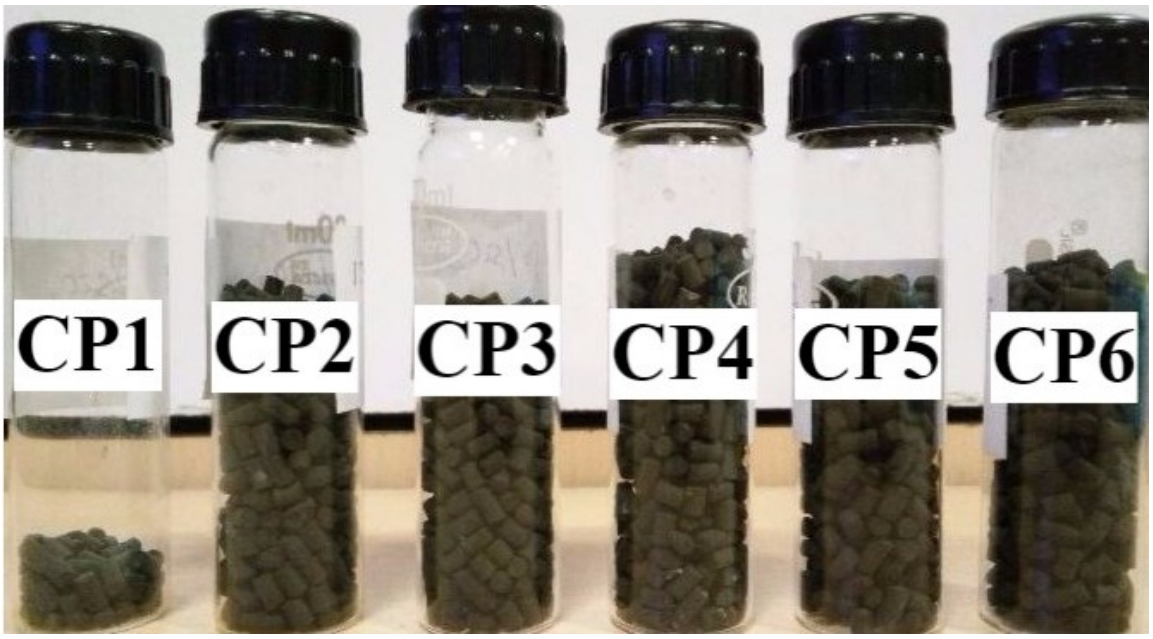

Figure 4.2: Calcined CP catalysts

4.2.1 Surface properties of CP catalysts

Surface area measurements revealed that the specific surface area of all the fresh six catalysts range between 117-139 m^2/g (as shown in Table 4.1). From the Table 4.1, comparing among CP1, CP2 and CP3 catalysts, it is visible that at every operation, surface modification or cobalt impregnation, made the catalyst surface area decrease. Correspondingly, the pore volume have become small, too. Also, incorporating 0.1% Pt to the same composition of CP1, CP2 and CP3, and preparing CP4, CP5 and CP6 catalysts, surface area increased, alongwith the same decreasing graph of surface area with increase in amount of Co content.

Table 4.1: Properties of CP catalysts

Catalyst	Surface area(m^2/g)	Total pore volume(cm^3/g)
CP1	138.72	0.487
CP2	130.34	0.437
CP3	120.16	0.416
CP4	128.44	0.430
CP5	122.57	0.415
CP6	117.52	0.382

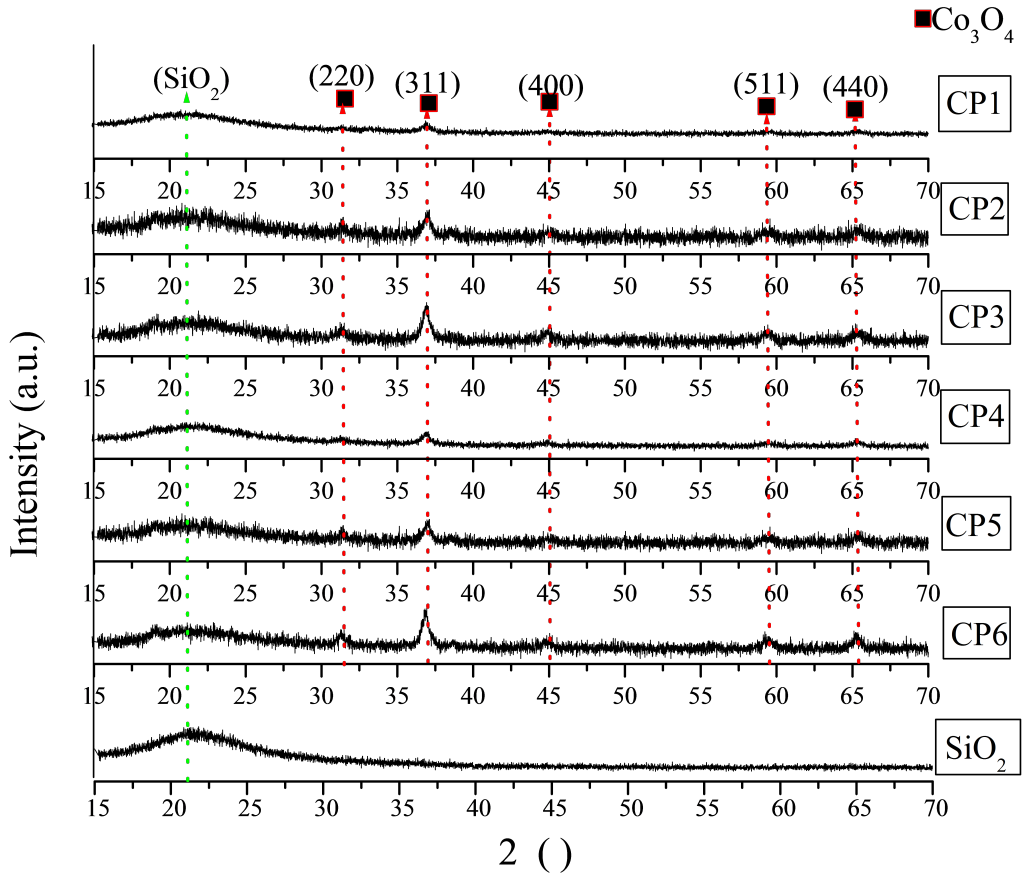

Figure 4.3: XRD images of calcined CP catalysts

4.2.2 Crystalline properties of CP catalysts

XRD patterns are shown in Fig. 4.3. All the samples showed Co_3O_4 phase of Co, identified by the diffraction peaks at 31.4°, 36.9°, 45.1°, 59.83° and 65.1° (Lucredio *et al.*, 2011). On the other hand, Pt incorporation didn't show any peak in this diffraction study, although presence of Pt has been confirmed other characterization studies. This may correspond to the idea of egg-shell catalyst formation in which Pt got induced inside the Co surface, just like egg white and egg yolk remains protected inside the eggshell.

4.2.3 Reducibility of CP catalysts

Table 4.2 shows the total amount of H_2 consumed by the CP catalysts. It is seen that that with increase in metal content, the amount of total H_2 consumption increases (comparing among CP1, CP2, CP3 and CP4, CP5, CP6). Also, an addition of 0.1% Pt

increased the H_2 consumption than it showed in catalysts without Pt (comparing CP4 to CP1, CP5 to CP2, and CP6 to CP3). Figure 4.4 shows TPR profiles for CP catalysts

Table 4.2: TPR data of the CP catalysts

Catalyst	Total H_2 consumption (μmol/g)
CP1	940.44
CP2	1890.69
CP3	2478.8
CP4	1067.06
CP5	2373.9
CP6	3152.2

where the profile for CP1 catalyst reveals that the first peak of its reduction is at 314°C and is attributed to the reduction of species Co^{3+} to $Co2^{2+}$. The second peak at 517°C identify the reduction of $Co^{2+} \rightarrow$ Co0. Besides these peaks, there is a third peak at 792°C referring to the reduction of Co species interacting more strongly with the SiO_2 support (Lucredio *et al.*, 2011). Next, the reduction behaviour of CP2 catalysts showed first peak at 316°C where Co^{3+} transformed to Co^{2+}, followed by two peaks at 392°C and 503°C where Co^{2+} to Co0 occured. The third peak was seen at 762°C which is lesser than the reduction temperature of the previous catalyst with lesser Co content.

Also, incorporating 0.1%Pt to the same composition of catalysts, reduction temperature was seen to get reduced (comparing graph of CP1 with CP4, CP2 with CP5 and CP3 with CP6).

4.2.4 Weight loss of CP catalysts

The TGA study on pre-calcined CP catalysts have been graphically shown in Fig. 4.5. An increase in weight loss has been seen comparing CP1 to CP2 to CP3 and similarly consecutive weight losses are visible from CP4 to CP5 to CP6. The same amount of Co content catalyst when incorporated with Pt have showed more weight loss.

4.2.5 Morphology of CP catalysts

The SEM images of all calcined CP catalysts have been shown in Fig. 4.6 which reveals that the geometry of the catalyst particles are not regular. Also, it is quite evident that the surfaces of the catalyst particles are not smooth.

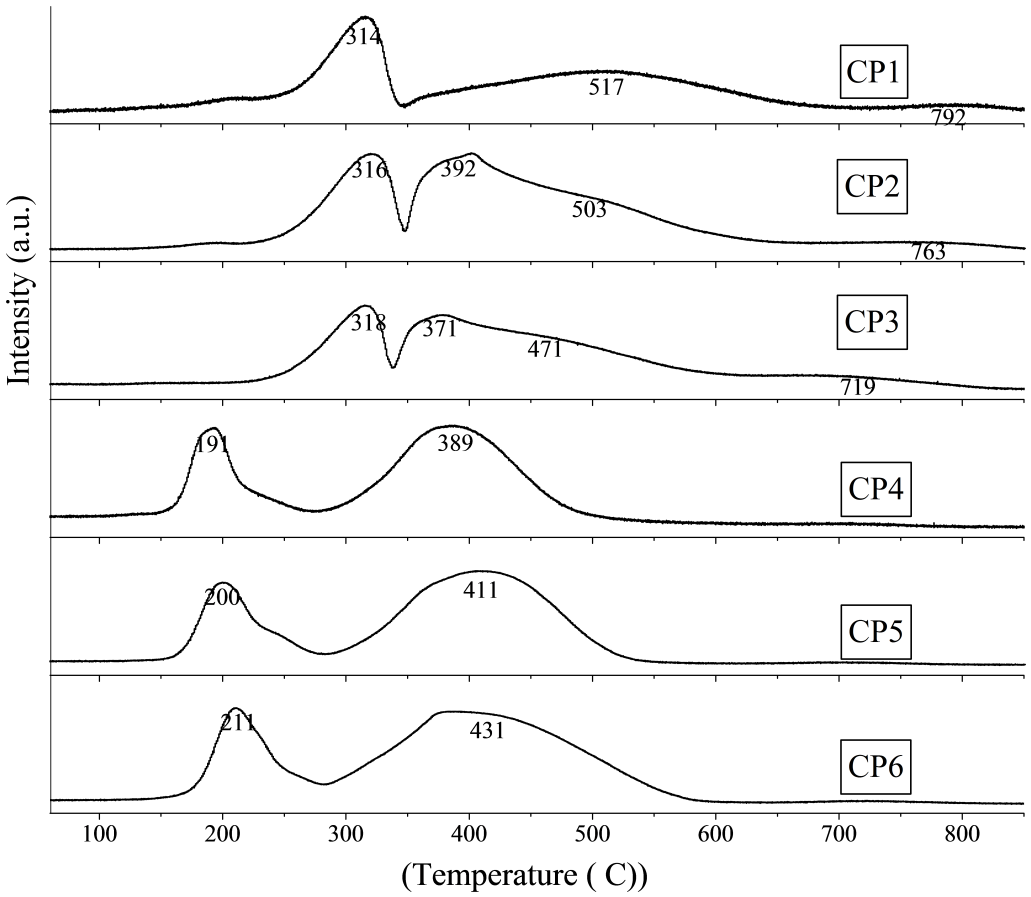

Figure 4.4: H_2-TPR profile of calcined CP catalysts

4.3 Activity of CP catalysts

4.3.1 Study on CP1 catalyst

From the Fig. 4.7, which shows the activity of CP1 catalyst, it is evident that, acetic acid conversion gradually increased with increase in temperature. Ethanol selectivity increased till 240°C, at which temperature it showed the highest selectivity, followed by gradual decrease in the same with more increase in temperature. Selectivity of ethyl acetate decreased till 240°C after which it got increased. Also, acetaldehyde selectivity was the highest at 260°C.

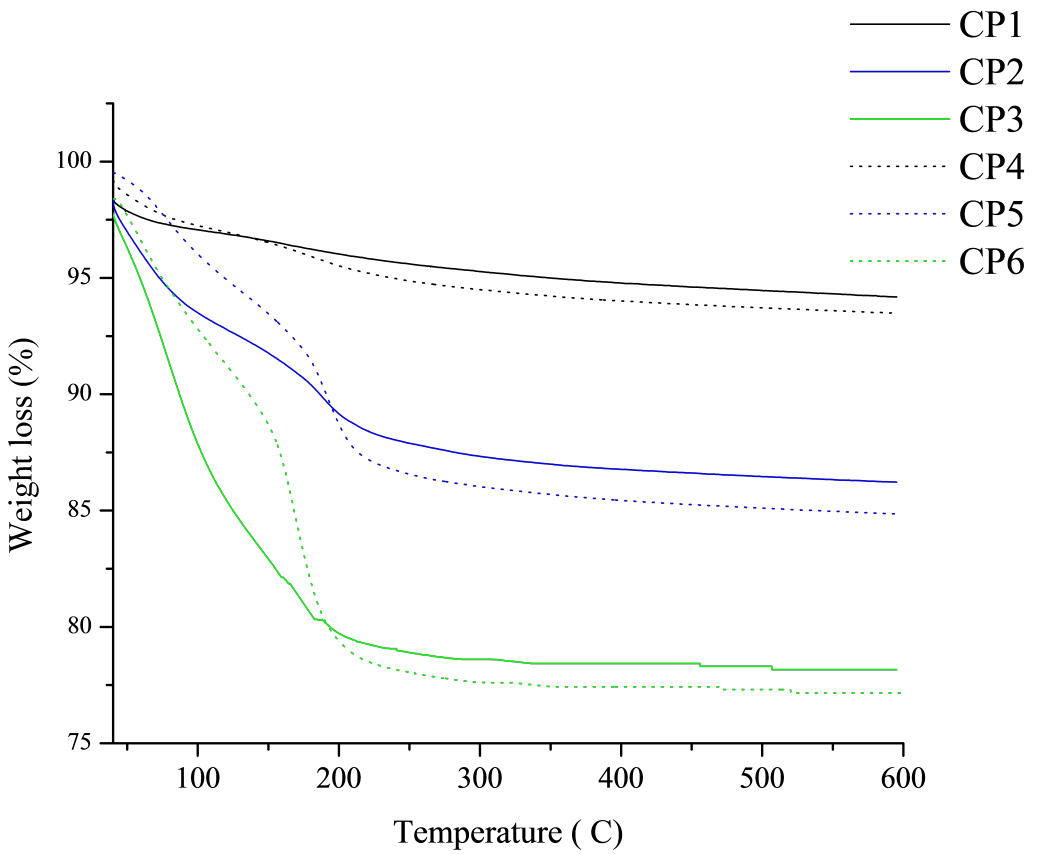

Figure 4.5: TGA profile of CP catalysts

4.3.2 Study on CP4 catalyst

The activity of CP4 catalysts are shown in Fig. 4.8. From this Fig., it is evident that ethanol selectivity was the highest at 240°C and it gradually decreased beyond this temperature. Acetic acid, on the other hand, showed gradual rise in its conversion with rise in temperature. Selectivity of ethyl acetate was same throughout the reaction temperature range of 220-320°C other than a reduced rate of the same at 240°C. Acetaldehyde selectivity was, although, very negligible at the beginning, but it increased a little with increase in temperature.

4.3.3 Study on CP6 catalyst

Fig. 4.9 shows the activity of CP6 catalysts, from which, is evident that, acetic acid conversion increased well with increase in the temperature. Ethanol selectivity was highest

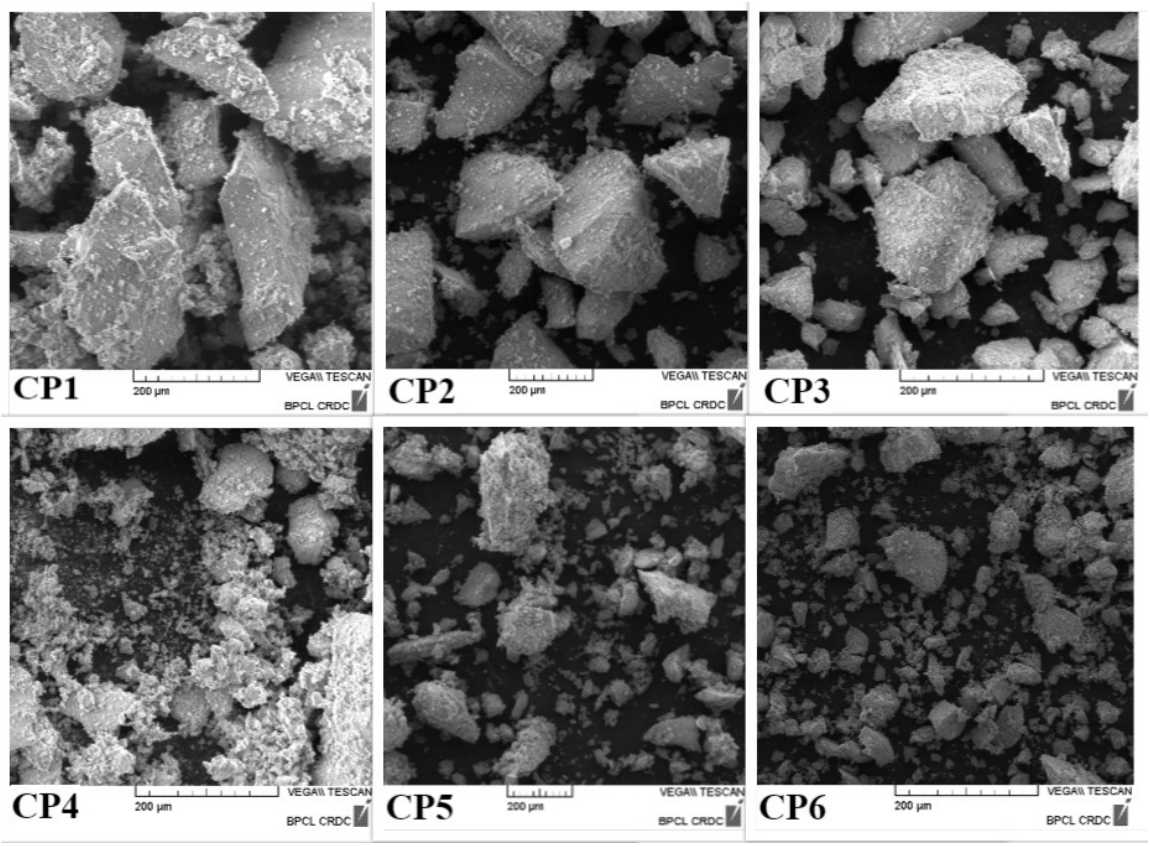

Figure 4.6: SEM images of calcined CP catalysts at 10kV

at 240°C after which it decreased at 260°C, followed by a gradual increase with further rise in the temperature. Selectivity of acetaldehyde and ethyl acetate was seen to be gradually decreasing and increasing respectively with increase in temperature.

4.3.4 Effect of CP catalysts in acetic acid hydrogenation to ethanol

At 240°C, all the three CP2, CP4 and CP6 catalysts showed their highest activities.Among these three CP catalysts, CP6 showed the highest acetic acid conversion and selectivity of ethanol at the same parameter conditions of fixed feed flow ratio at 240°C temperature and 20 bar pressure.

Table 4.3: Lab conversion data for CP1 catalyst

Run No.	T (°C)	Conversion (%)	Selectivity(%)		
			Ethanol	**Ethyl acetate**	**Acetaldehyde**
1	220	1.27	72.74	27.26	0
2	240	1.64	82.55	17.44	2.0
3	260	3.98	76.75	13.99	9.25
4	280	8.52	74.16	18.07	7.77
5	300	16.88	71.21	21.25	7.53
6	320	22.77	67.04	23	9.95

Table 4.4: Lab conversion data for CP4 catalyst

Run No.	T (°C)	Conversion (%)	Selectivity(%)		
			Ethanol	**Ethyl acetate**	**Acetaldehyde**
1	220	4.15	83.89	16.11	0
2	240	3.92	88.64	11.35	0
3	260	6.98	87.06	12.94	0
4	280	16.83	84.38	12.78	0.35
5	300	32.07	83.98	13.631	0.51
56	320	44.07	83.77	13.53	0.74

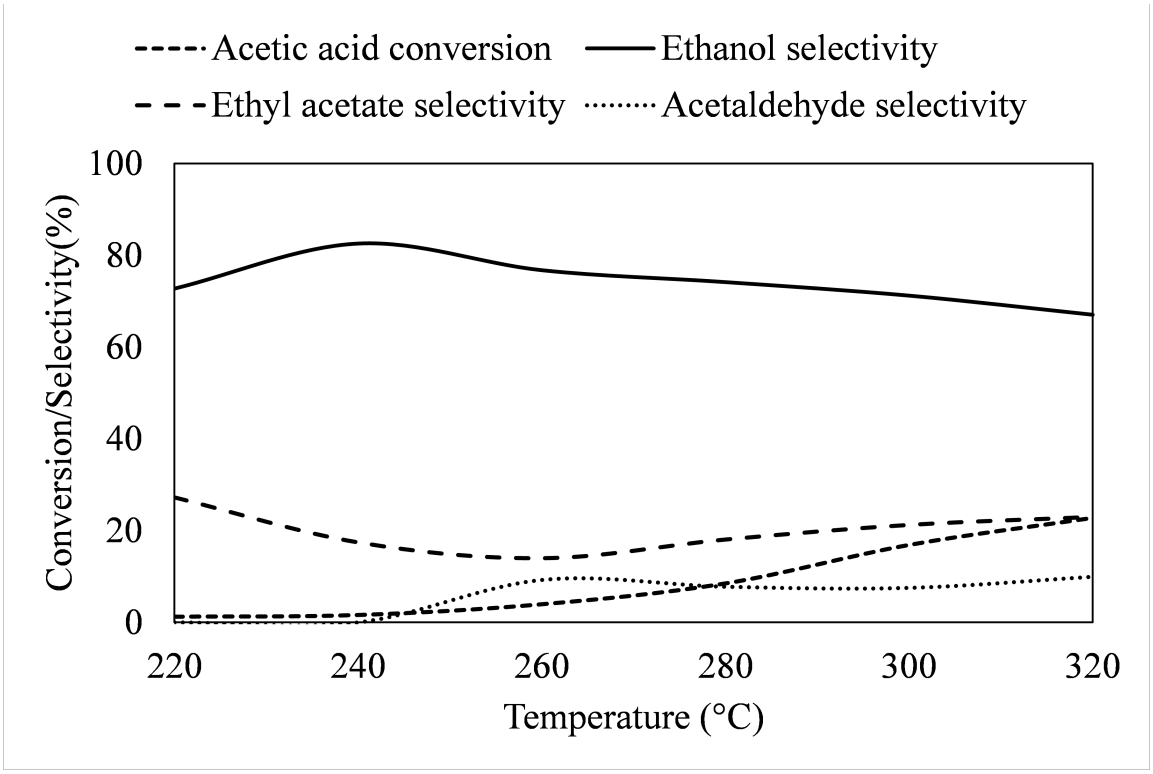

Figure 4.7: Effect of temperature on the performance of CP1 catalyst

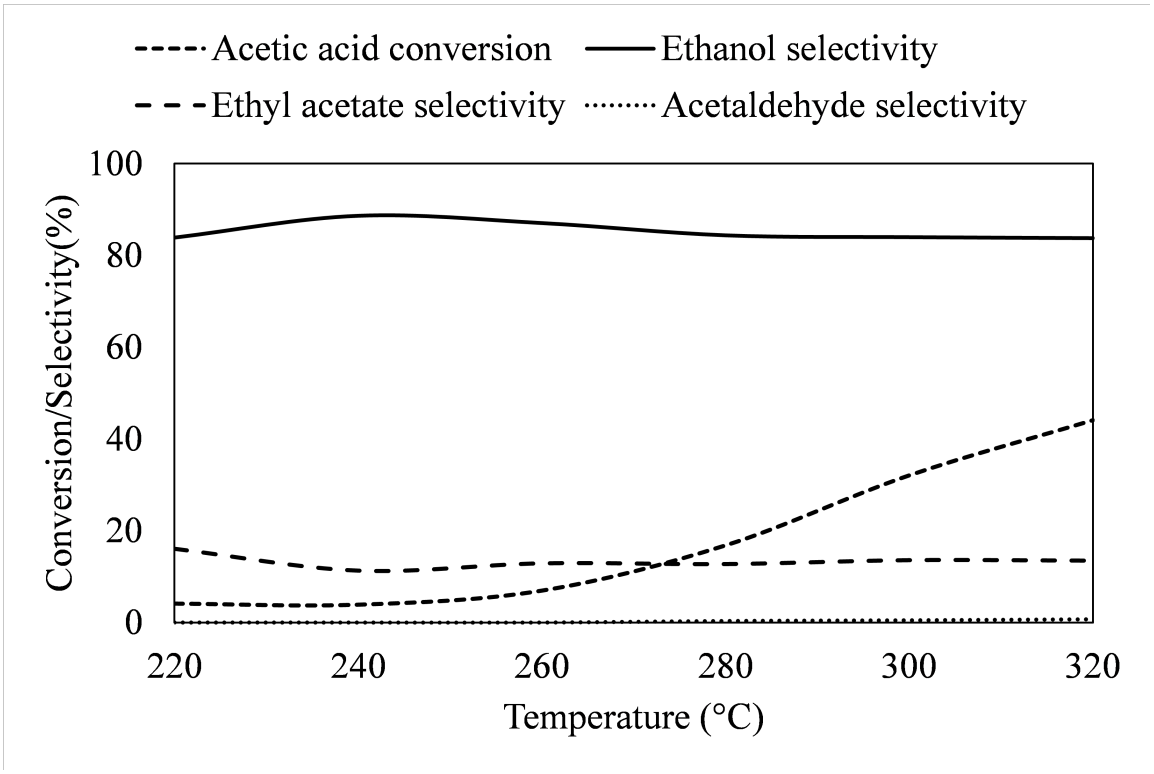

Figure 4.8: Effect of temperature on the performance of CP4 catalyst

Table 4.5: Lab conversion data for CP6 catalyst

Run No.	T (°C)	Conversion (%)	Selectivity(%)		
			Ethanol	**Ethyl acetate**	**Acetaldehyde**
1	220	13.37	90.58	9.41	0
2	240	22.52	92.56	7.43	0.10
3	260	29.38	91.46	7.95	0.59
4	280	41.0	92.00	6.78	1.20
5	300	51.616	92.27	6.08	1.63
6	320	60.11	92.46	5.75	1.78

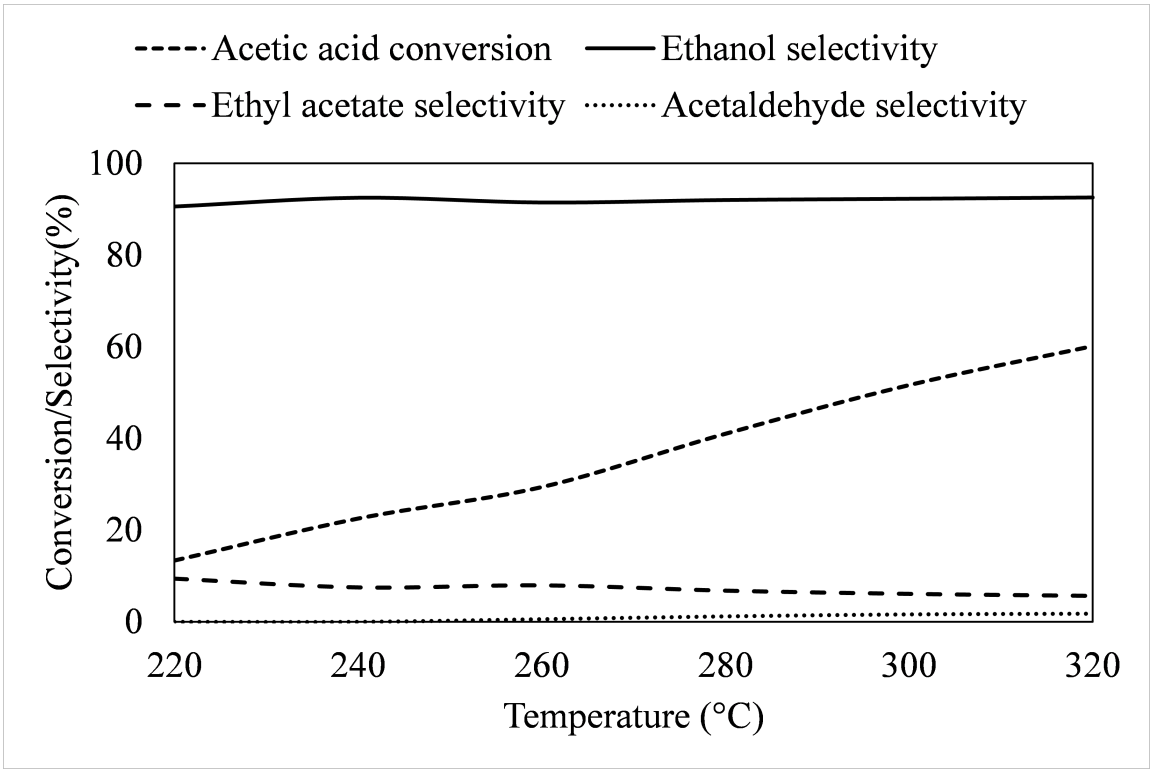

Figure 4.9: Effect of temperature on the performance of CP6 catalyst

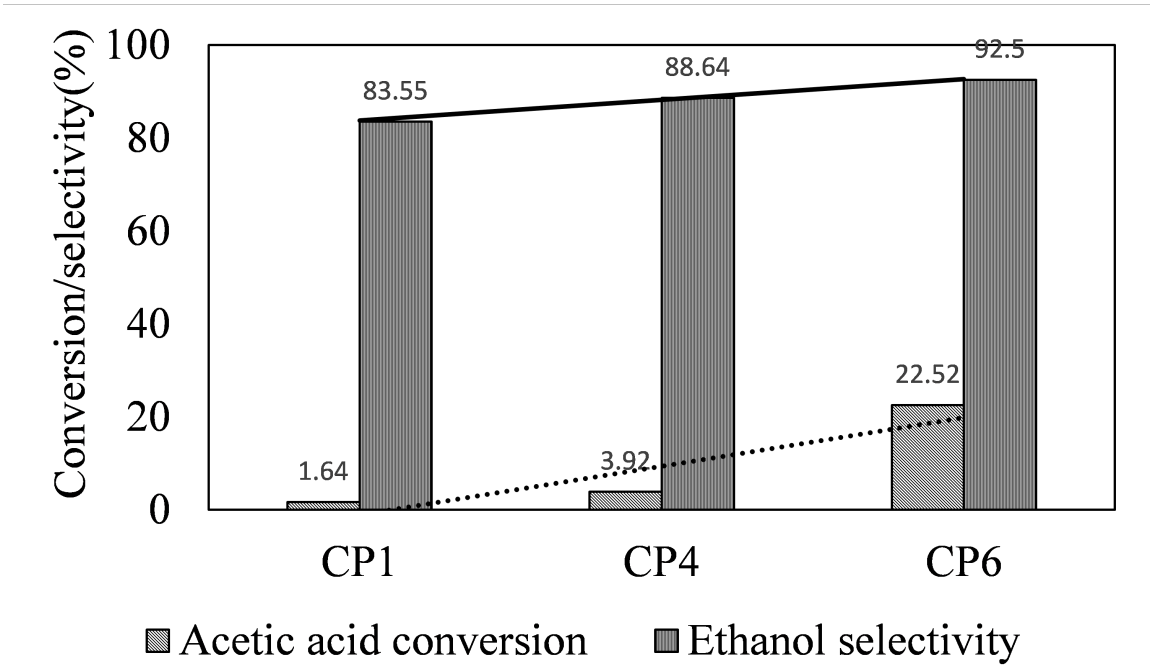

Figure 4.10: Comparison of activities among CP1, CP4 and CP6 catalysts at 240°C

CHAPTER 5

KINETICS ON ACETIC ACID CONVERSION TO ETHANOL

NOTE:The kinetics of CP catalysts are not completely in the present scope of the report. Hence an initial attempt has been done in the following chapter.

5.1 Catalyst preparation

SiO_2 supported Pt-Sn catalyst was prepared according to the same procedure as discussed in the section 3.3 of chapter 3.

The amounts of the metals present in this catalyst were: 2.1 Mol. wt.% platinum and 1.8 Mol. wt.% tin.

5.2 Study on catalyst activity

The activity of the catalyst was studied in the same experimental set up as mentioned in section 3.5 under the conditions discussed as follows.

Catalyst weight: 15 g

Pressure range: 1-20 bar g

Temperature range: 270-310°C

WHSV: 2-4/hr

Molar ratio of feeds (H_2:acetic acid): 3-5.

WHSV or Weight hourly space velocity is defined as the weight of feed flowing per unit weight of the catalyst per hour. Since weight of the catalyst charged into the reactor is not varied and always the same, so any variation in flow of feed per hour changes the WHSV.

The molar ratio of H_2 to acetic acid is the ratio between the amounts in moles of the two feed compounds involved in the reaction.

5.3 Performance of the catalyst

The reactions carried out at the conditions as shown in section 5.2 generated the results as tabulated in table 5.1.

Table 5.1: Lab conversion data of SiO_2 supported Pt-Sn catalyst

Run No.	T (°C)	P (bar)	WHSV (1/hr)	molar ratio of feed	Conversion (%)	Selectivity (water free basis)(%)		
						Ethanol	**Ethyl acetate**	**Acetal--dehyde**
1	270	1	3	7	20.9	60.5	19.8	19.7
2	290	1	3	7	24.1	53.9	23.6	22.5
3	310	1	3	7	34.4	49.2	25.2	25.6
4	270	10	2	7	47	89.9	8.6	1.6
5	270	10	3	7	39.9	91.7	6.9	1.4
6	270	10	4	7	31.4	94.2	5.1	0.7
7	270	10	3	3	33.6	36	62.7	1.3
8	270	10	3	5	36.9	52.2	46.5	1.3
9	270	20	3	7	56.7	94.4	4.8	0.8
10	290	10	3	7	43.6	76	22.7	1.3
11	310	10	3	7	47.9	72.5	25.9	1.6

5.3.1 Effect of temperature

As shown in the Fig. 5.1, the increase in temperature decreases the selectivity of ethanol although increases the conversion rate of acetic acid which again increases the selectivities of ethyl acetate and acetaldehyde.

5.3.2 Effect of WHSV

The effect of weight hourly space velocity (WHSV) on this reaction is shown in Fig. 5.2. It is evident that the increase in WHSV resulted to decrease in the conversion rate of acetic acid, whereas increased the selectivity rate of ethanol alongwith decreasing that of ethyl acetate and acetaldehyde.

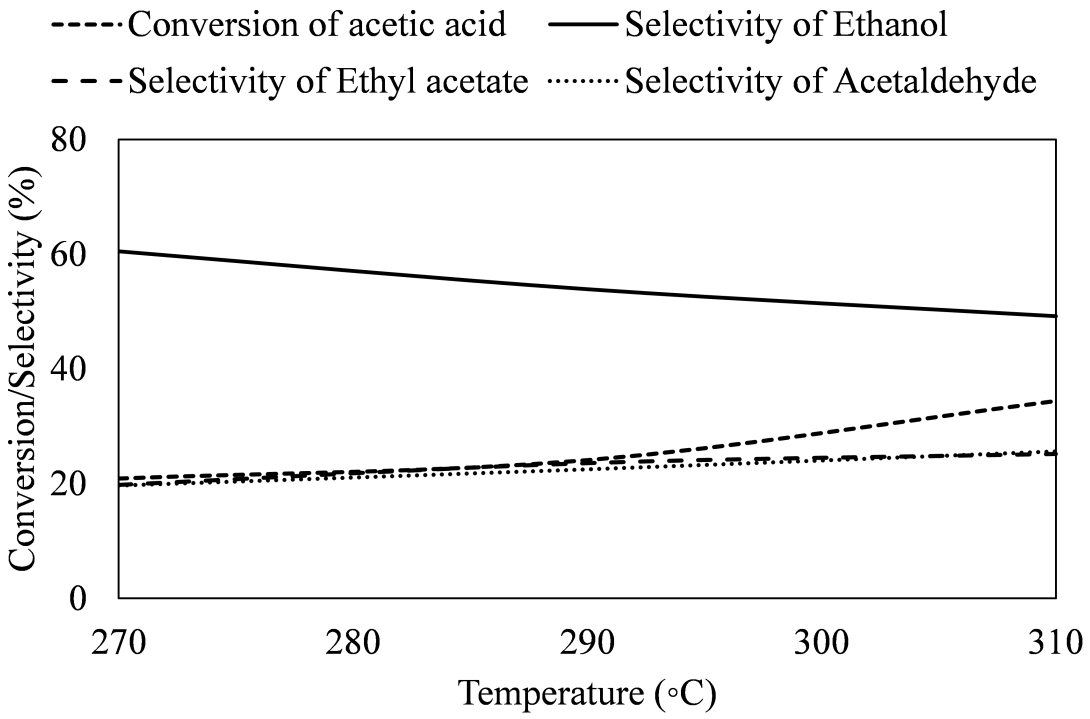

Figure 5.1: Effect of temperature on acetic acid conversion and products selectivity at P=1 bar, WHSV=3/hr, feed molar ratio=7

5.3.3 Effect of pressure

Increase in the pressure increased the conversion of acetic acid as well as the selectivity of ethanol, although the selectivity of ethyl acetate and acetaldehyde decreased.
Fig. 5.3 shows the effect of pressure on the conversion of acetic acid and selectivity of the products during this reaction.

5.3.4 Effect of molar ratio of feed

It is evident from the Fig. 5.4 that H_2/acetic acid molar ratio affects both the conversion of acetic acid and the selectivity of the products after the conversion. Increase in the H_2/Acetic acid molar ratio slightly increased conversion of acetic acid, but showed the highest rate of selectivity of ethanol. The selectivity of ethyl acetate decreased whereas that of acetaldehyde increased very minutely.

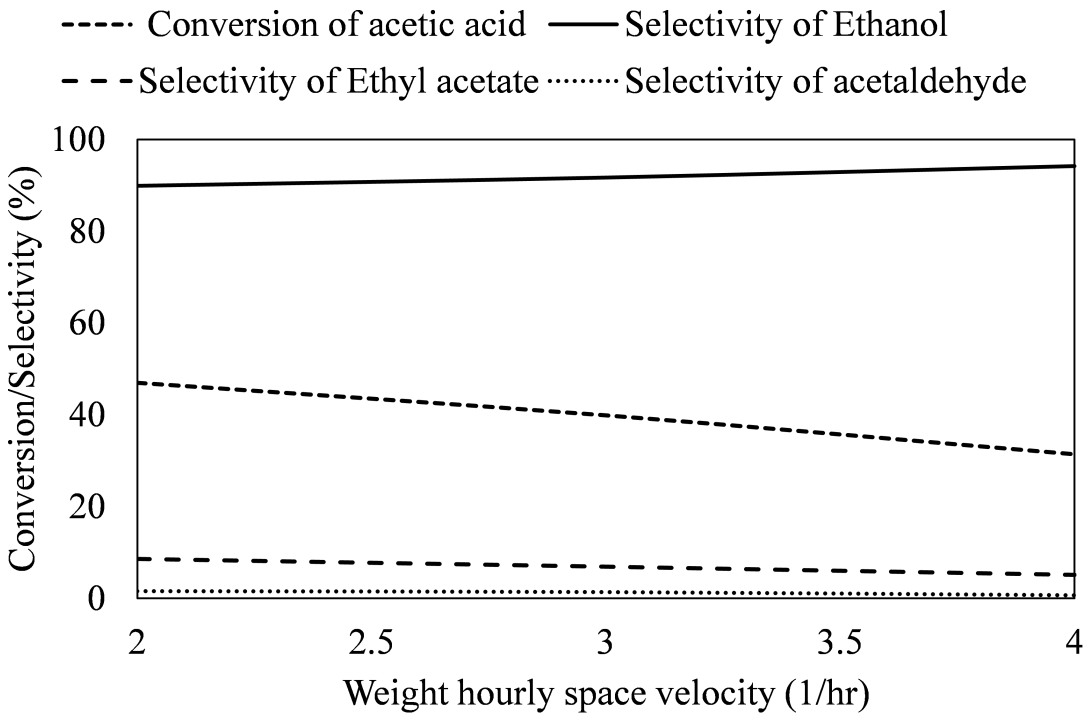

Figure 5.2: Effect of WHSV on acetic acid conversion and products selectivity at T=270°C, P=1 bar, feed molar ratio=7

5.4 Kinetic study

5.4.1 Determination of reaction rate expresssions

From the experimental data obtained, it is seen that acetic acid conversion is about 20-57% and with co-production of ethyl acetate and acetaldehyde, the selectivity of ethanol was the most notable. Thus the reactions which have been considered in this case are the hydrogenation of acetic acid to acetaldehyde, followed by its hydrogenation to ethanol and its esterification with acetic acid to ethyl acetate.

$$CH_3COOH + H_2 = CH_3CHO + H_2O \tag{5.1}$$

$$CH_3CHO + H_2 = C_2H_5OH \tag{5.2}$$

$$CH_3COOH + C_2H_5OH = CH_3CH_2COOCH_3 + H_2O \tag{5.3}$$

The fundamental steps involved in reaction 5.1 are sequentially represented by the Eqn. 5.4-5.7, that in reaction 5.2 are Eqn. 5.8-5.9 and in reaction 5.3 are Eqn. 5.10 - 5.11.

Concisely, Eqn. 5.4 represents the hydrogen dissociative adsorption, where * is an ac-

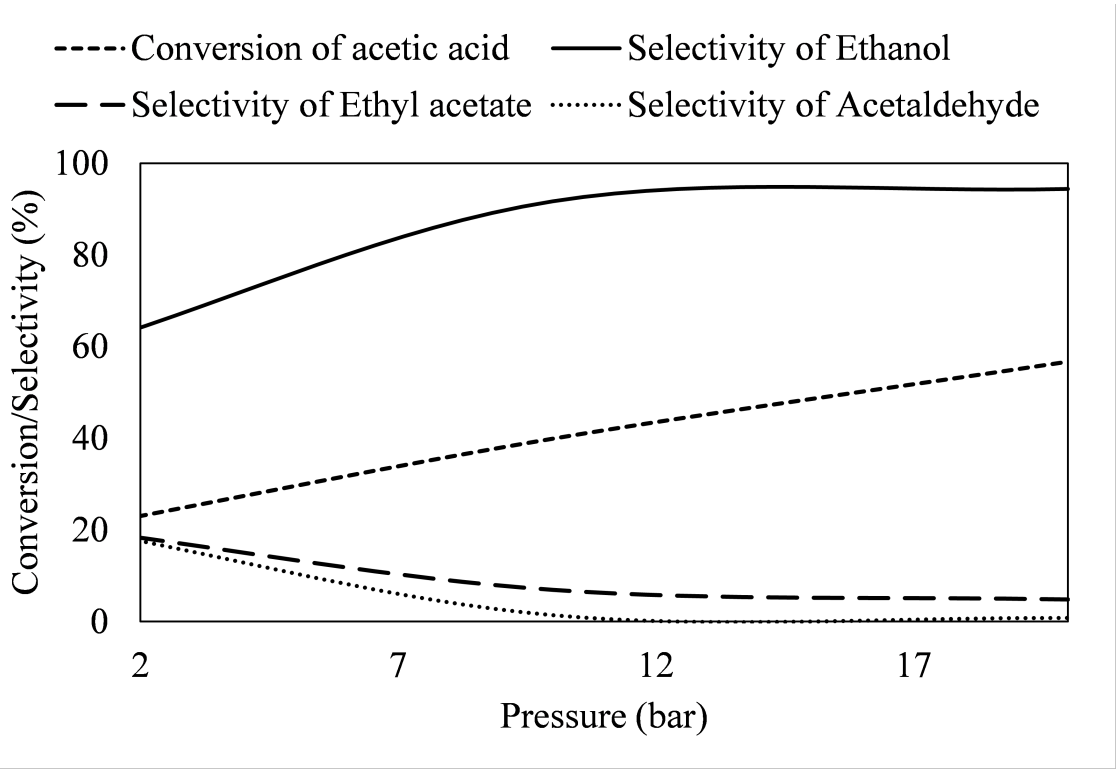

Figure 5.3: Effect of pressure on acetic acid conversion and products selectivity at T=270°C, WHSV=3/hr, feed molar ratio=7

tive site on the metal surface. Eqn. 5.5 shows the molecular acetic acid adsorption where S represents an oxide site surface is represented by S. With consecutive addition of hydrogen atoms adsorbed to the adsorbed acetic acid molecule, acetaldehyde is formed as the first product (as shown in Eqn. 5.6), which can desorb (Eqn. 5.7) or get converted to ethanol (Eqn. 5.8). Subsequently, the formed ethanol can desorb (Eqn. 5.9) or react with the adsorbed acetic acid molecule to form ethyl acetate (Eqn. 5.10). These surface reactions and reversible desorption stes are depicted by Eqns. 5.6-5.11 and the rate-determining steps of reactions 5.1, 5.2 and 5.3 are Eqns. 5.6, 5.8 and 5.10 respectively.

$$H_{2(g)} + 2^* \underset{k_{-1}}{\overset{k_1}{\rightleftharpoons}} 2H^* \tag{5.4}$$

$$CH_3COOH + S \underset{k_{-2}}{\overset{k_2}{\rightleftharpoons}} CH_3COOH - S \tag{5.5}$$

$$CH_3COOH - S + 2H^* \overset{K_3}{\rightarrow} CH_3CHO - S + H_2O + 2^* \tag{5.6}$$

$$CH_3CHO - S \underset{k_{-4}}{\overset{k_4}{\rightleftharpoons}} CH_3CHO + S \tag{5.7}$$

$$CH_3CHO - S + 2H^* \overset{K_5}{\rightarrow} CH_3CH_2OH - S + 2^* \tag{5.8}$$

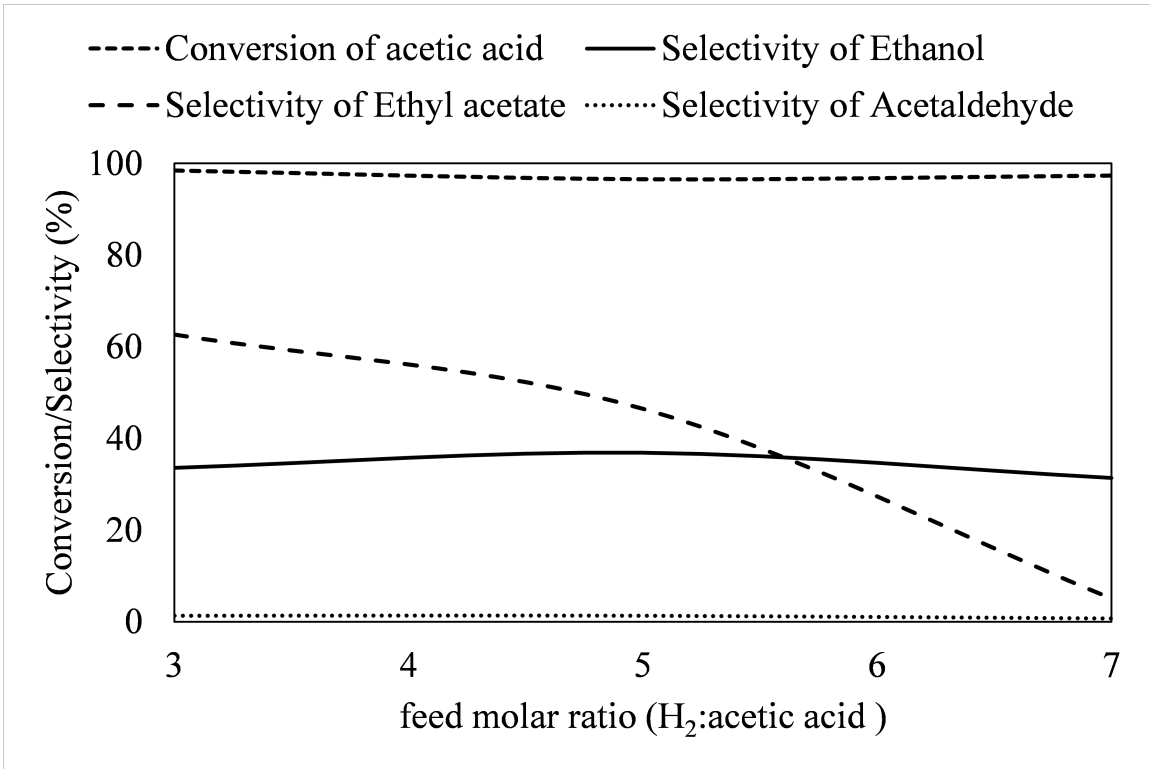

Figure 5.4: Effect of feed molar ratio (H_2:Acetic acid) on acetic acid conversion and products selectivity at T=270°C, P=10 bar, WHSV=3/hr

$$CH_3CH_2OH - S \underset{k_{-6}}{\overset{k_6}{\rightleftharpoons}} CH_3CH_2OH + S \tag{5.9}$$

$$CH_3CH_2OH - S + CH_3COOH - S \overset{K_7}{\rightarrow} CH_3COOC_2H_5 - S + S + H_2O \tag{5.10}$$

$$CH_3COOC_2H_5 - S \underset{k_{-8}}{\overset{k_8}{\rightleftharpoons}} CH_3COOC_2H_5 + S \tag{5.11}$$

The hydrogenation activities are considered as irreversible steps, and is determined by the rate of acetic acid disappeared to form hydrogenated products, i.e. the overall formation of rate of acetaldehyde (represented as r_1), ethanol (represented as r_2) and ethyl acetate (represented as r_3). Applying the steady-state approximation to the surface intermediates, the final rate expressions can be written as 5.12 - 5.15.

$$r_1 = K_3 \theta_{Ac-S} {\theta_{H*}}^2 \tag{5.12}$$

$$r_2 = K_5 \theta_{Act-S} {\theta_{H*}}^2 \tag{5.13}$$

$$r_3 = K_7 \theta_{Eth-S} \theta_{Ac-S} \tag{5.14}$$

where the fractional surface coverage of species i is denoted by θ_i, the adsorption of acetic acid, acetaldehyde and ethanol molecules on the oxide is shown by the subscripts Ac, Act and Eth respectively. The total number of active sites are combined in K_3, K_5 K_7.

The dissociative adsorption of hydrogen on the metal surface can be obtained from Eqn. 5.4 as:

$$k_1 P_{H_2} {\theta_*}^2 = k_{-1} {\theta_{H^*}}^2$$
$$\implies {\theta_{H^*}}^2 = \frac{k_1}{k_{-1}} P_{H_2} {\theta_*}^2$$
$${\theta_{H^*}}^2 = K_1 P_{H_2} {\theta_*}^2 \tag{5.15}$$

where,

$$K_1 = \frac{k_1}{k_{-1}}$$

It is assumed that under an environment filled with hydrogen, the weakly adsorbed molecular acetic acid the active intermediate in the reaction of hydrogenation, and adsorption acetic acid on the support is also assumed to be quasi-equilibrated, as depicted in Eqn. 5.5 in the sequence, where S is a site on the oxide surface.

$$k_2 \theta_S P_{Ac} = k_{-2} \theta_{Ac-S}$$
$$\implies \theta_{Ac-S} = \frac{k_2}{k_{-2}} \theta_S P_{Ac}$$
$$Or, \theta_{Ac-S} = K_2 \theta_S P_{Ac} \tag{5.16}$$

where,

$$K_2 = \frac{k_2}{k_{-2}}$$

Similarly, the quasi-equilibrated expression for acetaldehyde and ethanol adsorption can be represented as the following Eqn. 5.21 and Eqn. 5.23

$$k_4 \theta_{Act-S} = k_{-4} P_{Act} \theta_S$$
$$\implies K_4 = \frac{\theta_{Act-S}}{P_{Act} \theta_S} \tag{5.17}$$

$$And, k_6 \theta_{Eth-S} = k_{-6} P_{Eth} \theta_S$$
$$\implies K_6 = \frac{\theta_{Eth-S}}{P_{Eth} \theta_S} \tag{5.18}$$

$$[where, K_4 = \frac{k_{-4}}{k_4}; K_6 = \frac{k_{-6}}{k_6}]$$

According to the assumption of quasi-equilibrated H_2 adsorption on $_*$, the metal site bal-

ance can be represented as follows:

$$\theta_* + \theta_{H^*} = 1$$
$$\implies \theta_* = 1 - \theta_{H^*} = 1 - \theta_* \sqrt{K_1 P_{H_2}}$$
$$\implies \theta_*(1 + \sqrt{K_1 P_{H_2}}) = 1$$

$$Or, \theta_* = \frac{1}{1 + \sqrt{K_1 P_{H_2}}} \tag{5.19}$$

Quasiequilibrated acetic acid adsorption and formation of acetaldehyde, ethanol and ethyl acetate on S sites give

$$\theta_S + \theta_{Ac-S} + \theta_{Act-S} + \theta_{Eth-S} = 1$$
$$\implies \theta_S + K_2 \theta_S P_{Ac} + \frac{P_{Act}\theta_S}{K_4} + \frac{P_{Eth}\theta_S}{K_6} = 1$$
$$\implies \theta_S(1 + K_2 P_{Ac} + \frac{P_{Act}}{K_4} + \frac{P_{Eth}}{K_6}) = 1$$

$$\implies \theta_S = \frac{1}{(1 + K_2 P_{Ac} + \frac{P_{Act}}{K_4} + \frac{P_{Eth}}{K_6})} \tag{5.20}$$

Substituting Eqns. 5.15 - 5.20 into the reaction rate determining Eqns. 5.12 - 5.14 gives the final rate expressions (Eqn. 5.21 - 5.23) as follows:

$$r_1 = K_3(K_2 \theta_S P_{Ac})(K_1 P_{H_2} {\theta_*}^2) = \frac{K_1 K_2 K_3 P_{Ac} P_{H_2}}{(1 + \sqrt{K_1 P_{H_2}})^2 (1 + K_2 P_{Ac} + K_4 P_{Act} + K_6 P_{Eth})}$$

$$\implies r_1 = \frac{k_1 P_{Ac} P_{H_2}}{(1 + \sqrt{K_1 P_{H_2}})^2 (1 + K_2 P_{Ac} + K_4 P_{Act} + K_6 P_{Eth})} \tag{5.21}$$

$$r_2 5 = K_5 K_4 (P_{Act}\theta_S)(K_1 P_{H_2} {\theta_*}^2) = \frac{K_1 K_4 K_5 P_{Act} P_{H_2}}{(1 + \sqrt{K_1 P_{H_2}})^2 (1 + K_2 P_{Ac} + K_4 P_{Act} + K_6 P_{Eth})}$$

$$\implies r_2 = \frac{k_2 P_{Act} P_{H_2}}{(1 + \sqrt{K_1 P_{H_2}})^2 (1 + K_2 P_{Ac} + K_4 P_{Act} + K_6 P_{Eth})} \tag{5.22}$$

$$r_3 = K_7(K_6 \theta_{Eth-S} \theta_{Ac-S})(K_2 \theta_S P_{Ac}) = \frac{K_2 K_6 K_7 P_{Eth} P_{Ac}}{(1 + K_2 P_{Ac} + K_4 P_{Act} + K_6 P_{Eth})^2}$$

$$\implies r_3 = \frac{k_3 P_{Eth} P_{Ac}}{(1 + K_2 P_{Ac} + K_4 P_{Act} + K_6 P_{Eth})^2} \tag{5.23}$$

where,

$$k_1 = K_1 K_2 K_3 \tag{5.24}$$

$$k_2 = K_1 K_4 K_5 \tag{5.25}$$

$$k_3 = K_2 K_6 K_7 \tag{5.26}$$

k_1, k_2, k_3 are reaction rate constants. The dependence of these rate constants on temperature is expressed by the Arrhenius' law,

$$k_i = k_{0,i} exp(-E_{a,i}/RT), (i = 1, 2, 3) \tag{5.27}$$

while

$$K_i = exp(a_i + b_i/RT), (i = 1, 2, 4, 6) \tag{5.28}$$

5.4.2 Estimation of Kinetic parameters

Kinetic parameters of rate expressions developed (Eqn. 5.21 - 5.23) are estimated by matching the experimental results of Lab conversion data as shown in Table 6.1 with predicted results and their temperature dependence is determined by imposing an Arrhenius-type rate law (Eqn. 5.27 - 5.28). parameter estimation was done in MATLAB using *fminsearch*, which uses the simplex search method and finds the minimum of a scalar function of several variables, starting at an initial estimate.
The objective function chosen for minimizing the error between the experimental results and the predicted results is:

$$S = \sum \sum_{i=0}^{n} (f_0 - F_{outlet})^2 \tag{5.29}$$

5.4.3 Modeling of reactor

A fixed bed reactor model was further developed for the prediction of the reactor effluent yield.

Model assumptions:

The mathematical model for isothermal fixed-bed reactor is based on the following assumptions:

(1) The feed current in reactor shows plug flow behaviour and the gas phase is assumed

to behave ideally.

(2) The reactor is operated at steady state condition.

(3) Heat transfer from reactor to environment is negligible.

(4) The reactor is in isobaric operation.

(5) Radial gradients of concentration and temperature are absent.

$$\frac{dF_i}{dZ} = r(i) * \rho_{cat} * A \tag{5.30}$$

where, r(i)=reaction rate corresponding to formation or accumulation (mol/$g_{catalyst}$.hr) , i being the respective components

k_i=rate constants of surface reactions (mol/$g_{catalyst}$.hr) and K_i=adsorption constants of components (1/bar), as shown in Eqn. 5.27 - 5.28

F_i=flow rate (mol/hr)

$\rho_{catalyst}$=density of catalyst (g/m^3)

A=cross sectional area of reactor (m^2)

Z=reactor length (m)

X=acetic acid conversion

The ODE in the model can be solved using various analytical or numerical integration method. The numerical method is employed to solve this problem to avoid the rigorous implementation of analytical method. The reactor is assumed to be divided into small segments; properties of each segment is calculated from previous segment. The ODE in this model is solved using MATLAB which offers in-built function ODE45 based upon Runge-Kutta method.

5.5 Results and Discussion

5.5.1 Estimated values of the various kinetic parameters

The various estimated values of activation energy of the reactions and the other kinetic parameters are listed in Table 5.2.

Table 5.2: Estimated kinetic parameters

Parameter	Estimated value
$k_{1,0}$, (mol/$g_{catalyst}$.hr)	126
$E_{1,a}$, (J/mol)	-0.3589089
$k_{2,0}$, (mol/$g_{catalyst}$.hr)	6.3e-11
$E_{2,a}$ (J/mol)	-1.8527145
$k_{3,0}$ (mol/$g_{catalyst}$.hr)	1.31e-5
$E_{3,a}$ (J/mol)	-0.069976017
a_1	-248
b_1	-123
a_2	-7970
b_2	309
a_3	3860
b_3	-2740
a_4	-2.45
b_4	0.7664

5.5.2 Comparison between experimental conversion and simulated conversion

Comparisons of the predicted conversion at different operating conditions and the experimental data are shown in Fig. 5.5 and Table 5.3.

Table 5.3: Comparison study between experimental and simulated conversion

Run No.	T (°C)	P (bar)	WHSV (1/hr)	molar ratio of feed	Experimental conversion (%)	Simulated conversion (%)
1	270	1	3	7	20.9	19.29
2	290	1	3	7	24.1	23.47
3	310	1	3	7	34.4	28.58
4	270	10	2	7	47	58.73
5	270	10	3	7	39.9	50.72
6	270	10	4	7	31.4	45.43
7	270	10	3	3	33.6	46.96
8	270	10	3	5	36.9	49.53
9	270	20	3	7	56.7	64.70
10	290	10	3	7	43.6	58.09
11	310	10	3	7	47.9	66.80

The distribution of the points in the diagram indicates a reasonable good quality of fitness of the experimental data, by the kinetics Eqns. 5.21-5.23 with respect to the scope of the project; to get results near to the perfect fit, the number of experimental readings

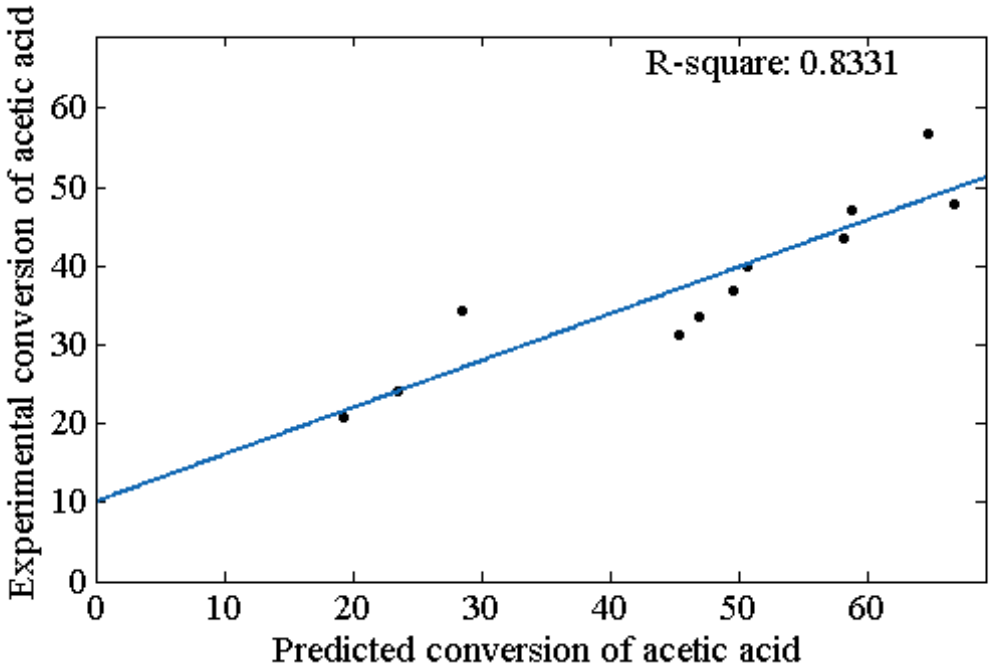

Figure 5.5: Experimental values of acetic acid conversion *versus* predicted values of acetic acid conversion

should be more. Therefore, the kinetic Eqns. 5.21-5.23 are suitable for this experiment.

5.5.3 Variation in the flow rates of feed and products along the reactor

Flow rates of acetic acid, acetaldehyde,ethanol and ethyl acetate at different depths of catalyst bed along the reactor at various temperatures (270 - 310°C) and 20 bar pressure, as calculated from the model are plotted in the above Figs. 5.6 - 5.8. From the figures, it is evident that acetic acid flow rate decreases along the reactor length and the products (acetaldehyde, ethanol and ethyl acetate) flow rates increase. The results also highlights the plug flow behaviour inside the reactor.

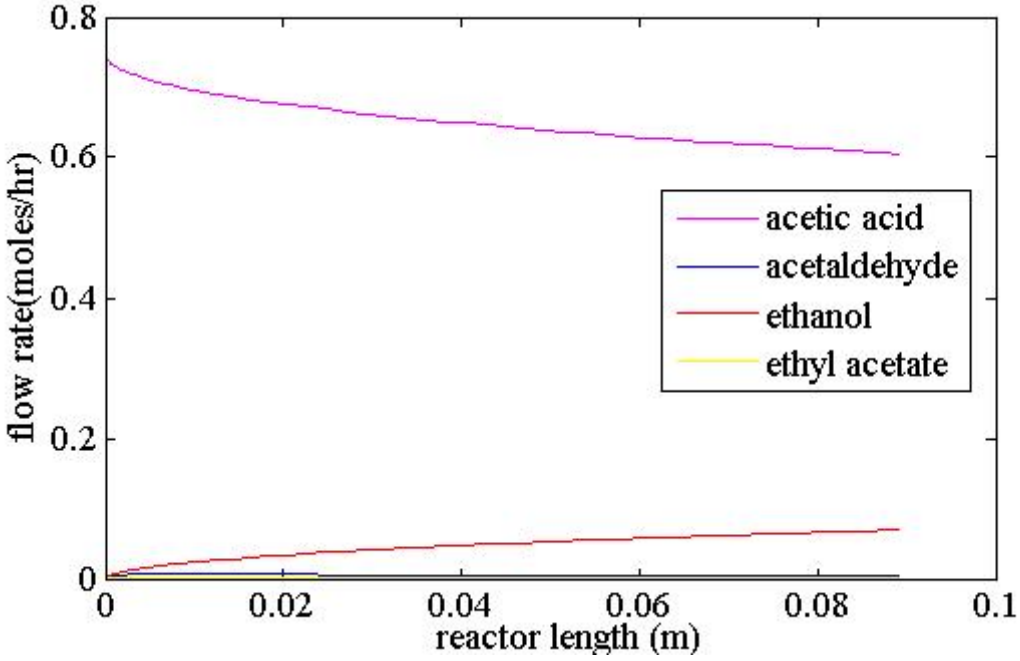

Figure 5.6: Variation of acetic acid, acetaldehyde,ethanol and ethyl acetate flow rates along the reactor at 270°C

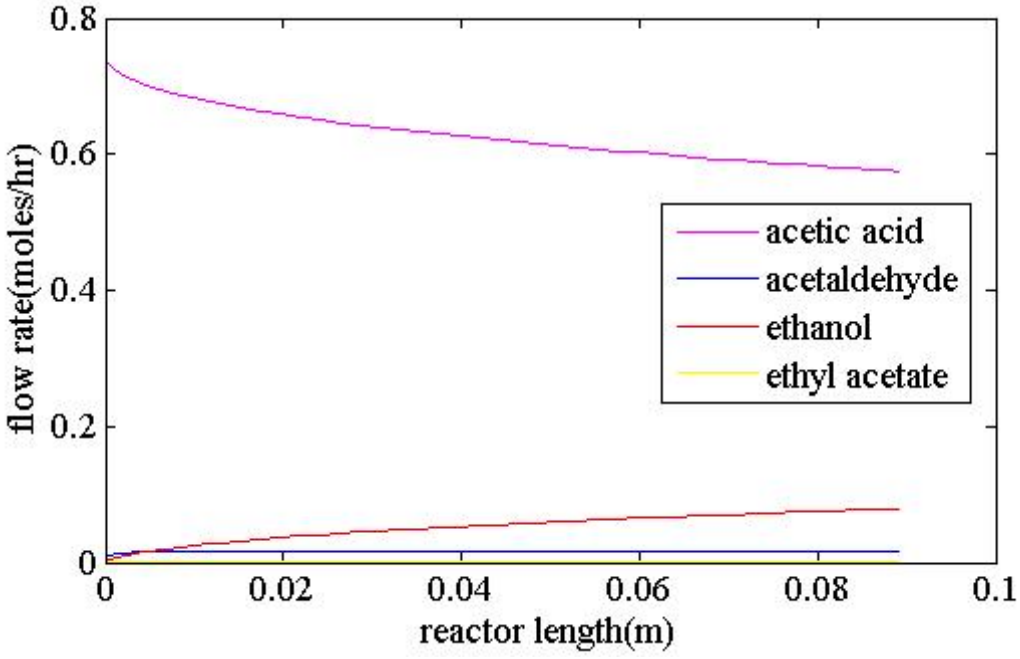

Figure 5.7: Variation of acetic acid, acetaldehyde,ethanol and ethyl acetate flow rates along the reactor at 290°C

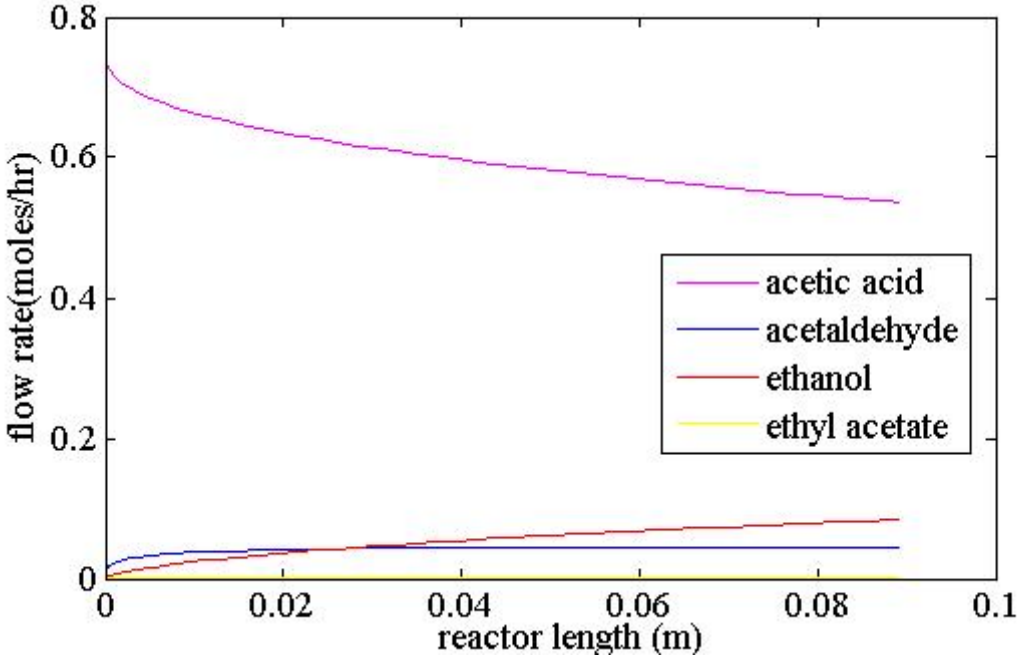

Figure 5.8: Variation of acetic acid, acetaldehyde, ethanol and ethyl acetate flow rates along the reactor at 310°C

CHAPTER 6

CONCLUSIONS

SiO_2-supported six catalysts consisting of Cobalt and Platinum with variation in their amounts were prepared and their characterization by BET, XRD, SEM, TGA and H_2-TPR were carried out. The characterization data suggests that the surface properties, pore volume, morphology, weight loss and reducibility of catalysts depend on the amounts of the metal contents in it. The catalytic effectiveness of these Co-Pt/SiO_2 catalysts were tested for acetic acid hydrogenation to ethanol keeping the feed flow rates constant on a fixed bed catalytic reactor at a temperature range varying from 220-320°C, at a constant pressure of 20 bar. The results showed a gradual increase in the conversion of acetic acid with the increase in the temperature.

For 5%Co/SiO_2, 5%Co-0.1%Pt/SiO_2 and 15%Co-0.1%Pt/SiO_2 catalysts, highest ethanol selectivity was seen at 240°C. With more rise in temperature, the ethanol selectivity gradually decreased in the presence of 5%Co/SiO_2 and 5%Co-0.1%Pt/SiO_2. In case of 15%Co-0.1%Pt/SiO_2 catalyst, ethanol selectivity, although gradually increased at first and showed its highest rate at 240°C, was seen to get reduced at 260°C; again, with more rise in temperature, a gradual increase in the same was observed.

Also, at 240°C, among these three catalysts, the highest selectivity of ethanol was seen in the presence of 15%Co-0.1%Pt/SiO_2 catalyst.

A kinetic expression for acetic acid conversion to ethanol in the form of Langmuir-Hinshelwood kinetics was generated based on elementary reactions that described the rate of ethanol synthesis with a good accuracy in a temperature range varying from 270-310°C in the presence of SiO_2 supported 2.1%Pt-1.8%Sn catalyst with minimum possible number of parameters. The other salient features that have been drawn from the study on this Pt-Sn/SiO_2 catalyst were:

(i) With the increase in temperature,the acetic acid conversion increased resulting to the increase in selectivity of ethyl acetate and acetaldehyde, whereas selectivity of ethanol decreased.

(ii) The increase in WHSV increased the selectivity rate of ethanol, whereas decreased the selectivity of ethyl acetate and acetaldehyde.

(iii) With the increase in the pressure, increase in both the conversion of acetic acid as well as the selectivity of ethanol was observed, although the selectivity of ethyl acetate and acetaldehyde decreased.

(iv) The increase in the feed molar ratio (ratio of H_2 to acetic acid) increased conversion of acetic acid, but showed the highest rate of selectivity of ethanol, but decreased that of ethyl acetate decreased showing a very minute increase in acetaldehyde selectivity.

REFERENCES

Alcala, R., **J. W. Shabaker**, **G. W. Huber**, **M. A. Sanchez-Castillo**, and **J. A. Dumesic** (2005). Experimental and DFT studies of the conversion of ethanol and acetic acid on PtSn-based catalysts. *Journal of Physical Chemistry B*, **109**(6), 2074–2085. ISSN 15206106.

Aly, M. and **E. Baumgarten** (2001). Hydrogenation of hexanoic acid with different catalysts. *Applied Catalysis A: General*, **210**(1-2), 1–12. ISSN 0926860X.

Chen, W. M., **Y. J. Ding**, **D. H. Jiang**, **T. Wang**, and **H. Y. Luo** (2006). A selective synthesis of acetic acid from syngas over a novel Rh nanoparticles/nanosized SiO2 catalysts. *Catalysis Communications*, **7**(8), 559–562. ISSN 15667367.

Choi, Y. and **P. Liu** (2009). Mechanism of ethanol synthesis from syngas on Rh(111). *Journal of the American Chemical Society*, **131**(36), 13054–13061. ISSN 00027863.

Fogler, H. S. (2006). Elements of chemical reaction engineering.

Ford, T. (1952). Preparation of alcohols from carboxylic acids. URL `http://www.google.co.in/patents/US2607807`. US Patent 2,607,807.

Fougret, C. M. and **W. F. Hölderich** (2001). Ethylene hydration over metal phosphates impregnated with phosphoric acid. *Applied Catalysis A: General*, **207**(1-2), 295–301. ISSN 0926860X.

Gong, J., **H. Yue**, **Y. Zhao**, **S. Zhao**, **L. Zhao**, **J. Lv**, **S. Wang**, and **X. Ma** (2012). Synthesis of ethanol via syngas on Cu/SiO 2 catalysts with balanced Cu 0-Cu + sites. *Journal of the American Chemical Society*, **134**(34), 13922–13925. ISSN 00027863.

Haider, M. A., **M. R. Gogate**, and **R. J. Davis** (2009). Fe-promotion of supported Rh catalysts for direct conversion of syngas to ethanol. *Journal of Catalysis*, **261**(1), 9–16. ISSN 00219517.

Howard, M. J., **M. D. Jones**, **M. S. Roberts**, and **S. A. Taylor** (1993). C1 to acetyls: catalysis and process. *Catalysis Today*, **18**(4), 325–354. ISSN 09205861.

Johnston, V., **B. Kimmich**, **J. van der Waal**, **J. Zink**, **V. Zuzaniuk**, **J. Chapman**, and **L. Chen** (2013). Ethanol production from acetic acid utilizing a cobalt catalyst. URL `http://google.com/patents/US20130184148`. US Patent App. 13/786,701.

Kiff, B. and **D. Schreck** (1983). Production of ethanol from acetic acid. URL `http://www.google.co.in/patents/US4421939`. US Patent 4,421,939.

Liu, Y., **K. Murata**, **M. Inaba**, **I. Takahara**, and **K. Okabe** (2011). Synthesis of ethanol from syngas over Rh/Ce1xZrxO2 catalysts. *Catalysis Today*, **164**(1), 308–314. ISSN 09205861. URL `http://linkinghub.elsevier.com/retrieve/pii/S0920586110007406`.

Lucredio, A., **J. Bellido**, **A. Zawadzki**, and **E. Assaf** (2011). Co catalysts supported on sio2 and -al2o3 applied to ethanol steam reforming: Effect of the solvent used in the catalyst preparation method. *Fuel*, **90**(4), 1424 – 1430. ISSN 0016-2361. URL `http://www.sciencedirect.com/science/article/pii/S0016236110006964`.

Miyake, T., **T. Makino**, **S. ichi Taniguchi**, **H. Watanuki**, **T. Niki**, **S. Shimizu**, **Y. Kojima**, and **M. Sano** (2009). Alcohol synthesis by hydrogenation of fatty acid methyl esters on supported Ru-Sn and Rh-Sn catalysts. *Applied Catalysis A: General*, **364**(1-2), 108–112. ISSN 0926860X.

Mustard, A. and **A. Aradhey** (2012). India Biofuels Annual 2012. *USDA Foreign Agriculture Service*, **15**, 1–16.

Olcay, H., **L. Xu**, **Y. Xu**, and **G. W. Huber** (2010). Aqueous-phase hydrogenation of acetic acid over transition metal catalysts. *ChemCatChem*, **2**(11), 1420–1424. ISSN 18673880.

Onyestyák, G., **S. Harnos**, **S. Klébert**, **M. Štolcová**, **A. Kaszonyi**, and **D. Kalló** (2013). Selective reduction of acetic acid to ethanol over novel Cu2In/Al2O3 catalyst. *Applied Catalysis A: General*, **464-465**, 313–321. ISSN 0926860X. URL http://www.sciencedirect.com/science/article/pii/S0926860X13003281.

Pallassana, V. (2002). Reaction Paths in the Hydrogenolysis of Acetic Acid to Ethanol over Pd(111), Re(0001), and PdRe Alloys. *Journal of Catalysis*, **209**, 289–305. ISSN 00219517. URL http://linkinghub.elsevier.com/retrieve/pii/S0021951702935852.

Pan, X., **Z. Fan**, **W. Chen**, **Y. Ding**, **H. Luo**, and **X. Bao** (2007). Enhanced ethanol production inside carbon-nanotube reactors containing catalytic particles. *Nature materials*, **6**(7), 507–511. ISSN 1476-1122.

Perego, C. and **P. Villa** (1997). Catalyst preparation methods. *Catalysis Today*, **34**, 281–305. ISSN 09205861.

Pestmam, R., **R. Koster**, **J. A. Z. Pieterse**, and **V. Ponec** (1997). Reactions of Carboxylic Acids on Oxides 2. Bimolecular Reaction of Aliphatic Acids to Ketones. *Journal of Catalysis*, **168**(2), 265–272. ISSN 00219517. URL http://www.sciencedirect.com/science/article/pii/S0021951797916249.

Rachmady, W. and **M. Vannice** (2002). Acetic Acid Reduction by H2 over Supported Pt Catalysts: A DRIFTS and TPD/TPR Study. *Journal of Catalysis*, **207**(2), 317–330. ISSN 00219517. URL http://www.sciencedirect.com/science/article/pii/S0021951702935566.

Rachmady, W. and **M. A. Vannice** (2000). Acetic acid hydrogenation over supported platinum catalysts. *Journal of Catalysis*, **192**(2), 322–334. ISSN 00219517. URL http://www.scopus.com/inward/record.url?eid=2-s2.0-0034631419{&}partnerID=40{&}md5=b2dd3dd05abe8c5fcf6bfbc2a383a5e1.

Rostrup-Nielsen, J. R. (2005). CHEMISTRY: Making Fuels from Biomass. *Science*, **308**(5727), 1421–1422. ISSN 0036-8075.

Solomon, B. D., **J. R. Barnes**, and **K. E. Halvorsen** (2007). Grain and cellulosic ethanol: History, economics, and energy policy. *Biomass and Bioenergy*, **31**(6), 416–425. ISSN 09619534.

Subramani, V. and **S. K. Gangwal** (2008). A review of recent literature to search for an efficient catalytic process for the conversion of syngas to ethanol. *Energy and Fuels*, **22**(2), 814–839. ISSN 08870624.

Sunley, G. J. and **D. J. Watson** (2000). High productivity methanol carbonylation catalysis using iridium - The Cativa (TM) process for the manufacture of acetic acid. *Catalysis Today*, **58**(4), 293–307. ISSN 0920-5861.

Verser, D. and **T. Eggeman** (2003). Process for producing ethanol. URL `http://www.google.co.in/patents/US6509180`. US Patent 6,509,180.

Xu, B. (1998). Rh/NaY: A selective catalyst for direct synthesis of acetic acid from syngas. *Journal of Catalysis*, **180**(2), 194–206. ISSN 00219517.

Yang, G., **X. San**, **N. Jiang**, **Y. Tanaka**, **X. Li**, **Q. Jin**, **K. Tao**, **F. Meng**, and **N. Tsubaki** (2011). A new method of ethanol synthesis from dimethyl ether and syngas in a sequential dual bed reactor with the modified zeolite and Cu/ZnO catalysts. *Catalysis Today*, **164**(1), 425–428. ISSN 09205861.

Zhang, S., **X. Duan**, **L. Ye**, **H. Lin**, **Z. Xie**, and **Y. Yuan** (2013). Supplementary Information for Production of ethanol by gas-phase hydrogenation of acetic acid over carbon nanotube-supported Pt Sn nanoparticles. *Catalysis Today*, **215**, 260–266.

APPENDIX 1

Estimation of kinetic parameters

```
function [g,x,Foutlet]=ACOH FUNC(x,Foutlet)
global parameterA parameterB Ti Pi
%pt=total pressure of reactor system in bar g
%Ti=temperature of reactor in K
%F1=flow rate of acetic acid in mol/hr
%F2=flow rate of hydrogen in mol/hr
%F3=flow rate of acetaldehyde in mol/hr
%F4=flow rate of ethanol in mol/hr
%F5=flow rate of water in mol/hr
%F6=flow rate of ethyl acetate in mol/hr
%Z=length of reactor in meter
%p(1)=partial pressure of acetic acid in bar
%p(2)=partial pressure of hydrogen in bar
%p(3)=partial pressure of acetaldehyde in bar
%p(4)=partial pressure of ethanol in bar
%p(5)=partial pressure of water in bar
%p(6)=partial pressure of ethyl acetate in bar
%r=reaction rate in mol/hr.g
%X=acetic acid conversion
F01=[0.74937552 5.245628643 0.0000001 0.0000001 0.0000001 0.0000001];
F02=[0.74937552 5.245628643 0.0000001 0.0000001 0.0000001 0.0000001];
F03=[0.74937552 5.245628643 0.0000001 0.0000001 0.0000001 0.0000001];
F04=[0.49958368 3.497085762 0.0000001 0.0000001 0.0000001 0.0000001];
F05=[0.74937552 5.245628643 0.0000001 0.0000001 0.0000001 0.0000001];
F06=[0.999167361 6.994171524 0.0000001 0.0000001 0.0000001 0.0000001];
F07=[0.74937552 2.248126561 0.0000001 0.0000001 0.0000001 0.0000001];
F08=[0.74937552 3.746877602 0.0000001 0.0000001 0.0000001 0.0000001];
F09=[0.74937552 5.245628643 0.0000001 0.0000001 0.0000001 0.0000001];
F10=[0.74937552 5.245628643 0.0000001 0.0000001 0.0000001 0.0000001];
```

```
F11=[0.74937552 5.245628643 0.0000001 0.0000001 0.0000001 0.0000001];
F0=[F01;F02;F03;F04;F05;F06;F07;F08;F09;F10;F11];
dim = size(x,2);
parameterA = x(1:dim/2);
parameterB = x(dim/2+1:dim);
T=[270 290 310 270 270 270 270 270 270 290 310]+273;
P=[1 1 1 10 10 10 10 10 20 10 10];
for i=1:11
F1=F0(i,:);
Ti = T(i);
Pi = P(i);
[t, F]=ode45( ACOH_FUNCN, [0 0.089],F1);
sz=size(F);
s=sz(1);
Foutlet(i,:)=F(s,:);
%X(i)=((F1(1)-Foutlet(i,1))/F1(1))*100;
end
Foutlet;
f01=[0.592756037 4.995937463 0.031694355 0.093071696 0.156619484 0.015926716];
f02=[0.56877602 4.969697988 0.041618081 0.095331154 0.1805995 0.021825133];
f03=[0.491590341 4.863895846 0.067447599 0.123947618 0.257785179 0.033194981];
f04=[0.264779351 3.052381982 0.003906835 0.20989945 0.23480433 0.010499022];
f05=[0.450374688 4.673481529 0.004361214 0.273146281 0.299000833 0.010746668];
f06=[0.685428809 6.385673562 0.0022907 0.294759411 0.313738551 0.00834422];
f07=[0.497585346 1.908270681 0.003325838 0.088065706 0.251790175 0.080199316];
f08=[0.472855953 3.329104092 0.003678975 0.141253943 0.276519567 0.065793324];
f09=[0.3244796 4.42065621 0.003545802 0.400076513 0.42489592 0.010636803];
f10=[0.422647794 4.673285027 0.004393794 0.245615889 0.326727727 0.038359022];
f11=[0.390424646 4.629672237 0.005931682 0.257005532 0.358950874 0.04800683];
f0=[f01;f02;f03;f04;f05;f06;f07;f08;f09;f10;f11];
%xexp=[20.9 24.1 34.4 47 39.9 31.4 33.6 36.9 56.7 43.6 47.9];
error=f0-Foutlet;
g=sum(sum(error.^2))
end

function f=ACOH_FUNCN(t,F)
global parameterA parameterB Ti Pi
```

```
Ft=F(1)+F(2)+F(3)+F(4)+F(5)+F(6);
P=Pi;
T=Ti;
p(1)=(F(1)/Ft)*P;
p(2)=(F(2)/Ft)*P;
p(3)=(F(3)/Ft)*P;
p(4)=(F(4)/Ft)*P;
p(5)=(F(5)/Ft)*P;
p(6)=(F(6)/Ft)*P;
K=(exp(parameterA(1:4)+parameterB(1:4)./((8.314*10^(-5))*T)));
k=parameterA(5:7).*exp(parameterB(5:7)./T);
r1=(k(1)*p(1)*p(2))/((1+(K(2)*p(1))+(K(3)*p(3))+(K(4)*p(4)))*((1+(K(1)*p(2))0.5)^2));
r2=(k(2)*p(3)*p(2))/((1+(K(2)*p(1))+(K(3)*p(3))+(K(4)*p(4)))*((1+(K(1)*p(2))0.5)^2));
r3=(k(3)*p(4)*p(1))/((1+(K(2)*p(1))+(K(3)*p(3))+(K(4)*p(4)))^2);
f(1,1)=(-r1-r3-r2)*0.272;
f(2,1)=(-r1-r2)*0.272;
f(3,1)=(r1-r2)*0.272;
f(4,1)=(r2-r3)*0.272;
f(5,1)=(r1+r3+r2)*0.272;
f(6,1)=(r3)*0.272;
end

clc
clear all
A=[4 4 4 4 4 4 4];
B=[1 0 1 0 1 1 1]; %starting guess at the solution
Parameters = [A B];
[Parameters,g]=fminsearch( ACOH_FUNC,Parameters);
[g,x]=ACOH FUNC(Parameters);
```

APPENDIX 2

Modeling of Reactor

```
function f=ACOH_FUNCN(t,F)
%pt=total pressure of reactor system in bar g
%Ti=temperature of reactor in K
%F1=flow rate of acetic acid in mol/hr
%F2=flow rate of hydrogen in mol/hr
%F3=flow rate of acetaldehyde in mol/hr
%F4=flow rate of ethanol in mol/hr
%F5=flow rate of water in mol/hr
%F6=flow rate of ethyl acetate in mol/hr
%t=length of catalyst in meter
%p(1)=partial pressure of acetic acid in bar
%p(2)=partial pressure of hydrogen in bar
%p(3)=partial pressure of acetaldehyde in bar
%p(4)=partial pressure of ethanol in bar
%p(5)=partial pressure of water in bar
%p(6)=partial pressure of ethyl acetate in bar
%r=reaction rate in mol/hr.g
%X=acetic acid conversion
Ft=F(1)+F(2)+F(3)+F(4)+F(5)+F(6);
P=Pi;
T=Ti;
p(1)=(F(1)/Ft)*P;
p(2)=(F(2)/Ft)*P;
p(3)=(F(3)/Ft)*P;
p(4)=(F(4)/Ft)*P;
p(5)=(F(5)/Ft)*P;
p(6)=(F(6)/Ft)*P;
K=(exp(parameterA(1:4)+parameterB(1:4)./(8.31*10^(-5)*T)));
k=parameterA(5:7).*exp(parameterB(5:7)./T);
```

```
r1=(k(1)*p(1)*p(2))/((1+(K(2)*p(1))+(K(3)*p(3))+(K(4)*p(4)))*((1+(K(1)*p(2))^(0.5))^2));
r2=(k(2)*p(3)*p(2))/((1+(K(2)*p(1))+(K(3)*p(3))+(K(4)*p(4)))*((1+(K(1)*p(2))^(0.5))^2));
r3=(k(3)*p(4)*p(1))/((1+(K(2)*p(1))+(K(3)*p(3))+(K(4)*p(4)))^2);
f(1,1)=(-r1-r3-r2)*0.272;
f(2,1)=(-r1-r2)*0.272;
f(3,1)=(r1-r2)*0.272;
f(4,1)=(r2-r3)*0.272;
f(5,1)=(r1+r3+r2)*0.272;
f(6,1)=(r3)*0.272;
end


function    [g,Foutlet,Conv]=ACOH_FUNC(x)
global parameterA parameterB Ti Pi
F01=[0.74937552 5.245628643 0.0000001 0.0000001 0.0000001 0.0000001];
F02=[0.74937552 5.245628643 0.0000001 0.0000001 0.0000001 0.0000001];
F03=[0.74937552 5.245628643 0.0000001 0.0000001 0.0000001 0.0000001];
F04=[0.49958368 3.497085762 0.0000001 0.0000001 0.0000001 0.0000001];
F05=[0.74937552 5.245628643 0.0000001 0.0000001 0.0000001 0.0000001];
F06=[0.999167361 6.994171524 0.0000001 0.0000001 0.0000001 0.0000001];
F07=[0.74937552 2.248126561 0.0000001 0.0000001 0.0000001 0.0000001];
F08=[0.74937552 3.746877602 0.0000001 0.0000001 0.0000001 0.0000001];
F09=[0.74937552 5.245628643 0.0000001 0.0000001 0.0000001 0.0000001];
F10=[0.74937552 5.245628643 0.0000001 0.0000001 0.0000001 0.0000001];
F11=[0.74937552 5.245628643 0.0000001 0.0000001 0.0000001 0.0000001];
F0=[F01;F02;F03;F04;F05;F06;F07;F08;F09;F10;F11];
dim = size(x,2);
parameterA = x(1:dim/2);
parameterB = x(dim/2+1:dim);
T=[270 290 310 270 270 270 270 270 270 290 310]+273;
P=[1 1 1 10 10 10 10 10 20 10 10];
for i=1:11
figure(i);
clf(i);
F1=F0(i,:);
Ti = T(i);
Pi = P(i);
```

```
[t,F]=ode45(@ACOH_FUNCN, [0 0.089],F1);
sz=size(F);
plot(t,F(:,1)); hold on
plot(t,F(:,2)); hold on
plot(t,F(:,3)); hold on
plot(t,F(:,4)); hold on
plot(t,F(:,5)); hold on
plot(t,F(:,6)); hold on
s=sz(1);
Foutlet(i,:)=F(s,:);
Conv(i)=((F1(1)-Foutlet(i,1))/F1(1))*100;
end
end
```